←Quantum

Beam splitter

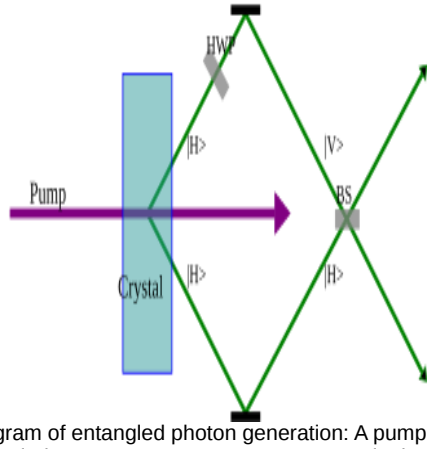

Diagram of entangled photon generation: A pump beam induces type-I spontaneous parametric down-conversion (SPDC) in a nonlinear crystal, producing a polarization-entangled photon pair (signal and idler modes). The pair is input to a 50:50 beam splitter,700-1100nm (https://www.thorlabs.com/non-polarizing-cube-beamsplitters-700---1100-nm?tabName=Overview)creating path-entangled output modes for quantum experiments like Bell tests.

Other names	BS, directional coupler (in waveguide form)
Primary uses	Quantum superposition · Entanglement generation · Photon statistics · Hong–Ou–Mandel interferometry · Linear-optical quantum computing · Quantum metrology · Quantum communication

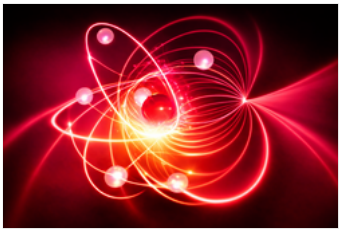

Artistic impression of an atom 8

Theory for the beam splitter in quantum optics

Theory for the beam splitter (BS) in quantum optics, quantum entanglement of photons and their statistics, the HOM effect, is well developed and based on fairly simple mathematical and physical foundations. This theory has been developed for any type of BS and is based on the constancy of the reflection coefficients R (or the transmission coefficient, where R + T = 1) and the phase shift ϕ. The constancy of these coefficients cannot always be satisfied for a waveguide BS, where R and ϕ depend in a special way on photon frequencies. Based on this, the concept of BS systematizes in quantum optics into "Conventional" and frequency-dependent BS, and also confirms the theory of such BS.The quantum entanglement, photon statistics at the output ports, and the Hong-Ou-Mandel (HOM) effect for such BS can be very different. Taking into account the fact that the waveguide BS is currently acquiring an important role in quantum technologies due to the possibility of its miniaturization, this article will be useful not only for theoreticians, but also for experimenters.

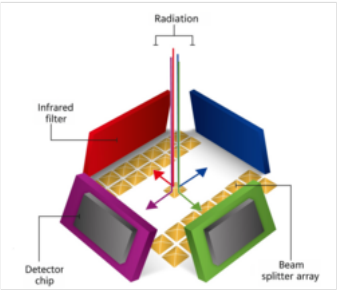

Schematic diagram of a reflection beam splitter in a pyroelectric infrared detector (four optical channels)"

Historical developments in beam splitting range from **Fizeau's 1851**[30] interference measurements to the development of the **Michelson interferometer**. The transition to the quantum regime occurred in 1987 with the first experimental demonstration of the HOM effect.[34] The KLM protocol(2001) demonstrated that universal linear optical quantum computing is possible by using only beam splitters, phase shifters, and single-photon detectors.It uses a process called Measurement-Induced Nonlinearity.[27][36]

Recent years

Have witnessed significant progress in quantum communication and quantum internet with the emerging quantum photonic chips, whose characteristics of scalability, stability, and low cost, open up new possibilities in miniaturized essentials. This provides an overview of the advances in quantum photonic chips for quantum communication, beginning with a summary of the prevalent photonic integrated fabrication platforms and key components for integrated quantum communication systems. Then discusses a range of quantum communication applications, such as quantum key distribution and quantum teleportation. Finally, the review culminates with a perspective on challenges towards high-performance chip-based quantum communication, as well as a glimpse into future

Keywords:

Beam splitter, Integrated photonics, Quantum information,waveguide beam splitter, quantum entanglement, photons, reflection coefficient, phase shift, photon statistics, Hong-Ou-Mandel effect.

Schematic of the Hong–Ou–Mandel effect: Two indistinguishable photons incident on a 50:50 beam splitter exhibit quantum interference, leading to photon bunching (both photons exit the same port).On-chip HOM interference visibilities exceeding 0.97 were observed using independent molecular sources. [1] Additionally, quantum beating was observed when a frequency detuning was applied between two molecules, persisting for over 100 μs. [2]

Quantum optical classifier

Superexponential speedup classification is a central task in deep learning algorithms. Usually, images are first captured and then processed by a sequence of operations, of which the artificial neuron represents one of the fundamental units. This paradigm requires significant resources that scale (at least) linearly in the image resolution, both in terms of photons and computational operations. Present is a quantum optical pattern recognition method for binary classification tasks. It classifies objects without reconstructing their images, using the rate of two-photon coincidences at the output of a Hong-Ou-Mandel interferometer, where both the input and the classifier parameters are encoded into single-photon states. This method exhibits the behaviour of a classical neuron of unit depth. Once trained, it shows a constant $\mathcal{O}(1)$ complexity in the number of computational operations and photons required by a single classification. This is a superexponential advantage over a classical artificial neuron.

On-chip integration

Of independent channels of indistinguishable single photons is a prerequisite for scalable optical quantum information processing. This requires separate solid-state single-photon emitters to exhibit identical lifetime-limited transitions. This challenging task is usually further exacerbated by spectral diffusion due to complex charge noise near material surfaces made by nanofabrication processes. A molecular quantum photonic chip that demonstrate on-chip Hong–Ou–Mandel quantum interference of indistinguishable single photons from independent molecules is developed. The molecules are embedded in a single-crystalline organic nanosheet and integrated with single-mode waveguides without nanofabrication, thereby ensuring stable, lifetime-limited transitions. With the aid of Stark tuning, 100 waveguide-coupled molecules can be tuned to the same frequency and achieve on-chip Hong–Ou–Mandel interference visibilities exceeding 0.97 for 2 molecules separately coupled to 2 waveguides. For two molecules with a controlled frequency difference, over 100-μs-long quantum beating in the interference, showing both excellent single-photon purity (particle nature) and long coherence (wave nature) of the emission.The results show a possible strategy towards constructing scalable optical universal quantum processors and a promising platform for studying waveguide quantum electrodynamics with identical single emitters wired via photonic circuits.

Integrated Photonics in Quantum Technologies

Integrated photonics in quantum technologies [197][198]. The advantages of single-photon state encoding are several and include the lack of decoherence phenomena, the possibility to realize information processing at room temperature and to send photons through fibers and free space channels. In the last ten years, improvements in photonic quantum technologies enabled an increase in the complexity of the implemented system, supporting relevant advances in various branches of quantum information, including the demonstration of quantum advantage [199][200][201] and satellite quantum communications [202][203].
Indistinguishable single photons are a fundamental resource for optical quantum technologies[3][4][1], underpinning universal quantum computing, quantum simulation and quantum networks. Although recent demonstrations of some preliminary quantum photonic applications primarily rely on parametric-process-based single-photon sources[2][5], deterministic sources offer greater future promise[4][6][7][8][9]. Solid-state single-quantum emitters, such as quantum dots[4][9], colour centres[10][11][12][13] and organic molecules[14][15], could serve as a versatile platform

Overview

Quantum states of light are basic resources for the realization of quantum information processing tasks, starting from pioneering experiments of quantum non-locality and quantum teleportation[110][111] and extending to modern quantum communication and computation efforts. The transition from bulk optics to integrated photonic circuits has been essential for scaling these technologies, enabling the miniaturization of complex interferometric networks on a single chip. The advantages of single-photon encoding include resistance to decoherence effects, the possibility of operation in an ambient temperature environment, and the ability to transfer photons via an optical fiber as well as free space communication links. The last decade has marked a growing complexity of photonic quantum technology efforts that have made possible the enhancement of quantum advantage experiments[198][199][200] and quantum communication via satellites [201][202]

An essential enabling technology in these advances is the coupling of photonic device components supporting the generation, manipulation, and detection of quantum states [203][204][205]. On-chip integration of independent channels of indistinguishable single photons is a prerequisite for scalable optical quantum information processing. Integrated photonics enables the realization of waveguides and reconfigurable optical components, which in turn make possible multi-port reprogrammable optical networks, and most recently, integrated processors merging both quantum state preparation and quantum processing. A molecular quantum photonic chip has been developed, demonstrating on-chip Hong–Ou–Mandel quantum interference of indistinguishable single photons emitted from independent molecules..This requires separate solid-state single-photon emitters to exhibit identical lifetime-limited transitions.While the integration of single-photon detectors is still a challenge, some very promising advances have been made in recent years towards fully integrated photonic platforms. Compared to conventional discrete optical platforms, which demand a very careful alignment of discrete components, experience stability problems, and face cost scalability, quantum photonic chips on a microchip offer advantages in miniaturization, scalability, stability, and potentially low cost mass production. In this sense, quantum photonic chips constitute a highly promising platform for applied quantum communication, specifically in quantum key distribution (QKD), quantum secure direct communication, quantum teleportation[247][219] , and, in general, in quantum networks.

designing scaled-down and scalable quantum optical components, a thorough understanding of both conventional and frequency-dependent beam splitters is necessary for carrying out experiments in integrated quantum communication.

An interactive simulation of quantum teleportation in the Virtual Lab by Quantum Flytrap, (https://lab.quantumflytrap.com/lab/quantum-teleportation?mode=waves)

History

Key milestones:

- 1851: The Fizeau experiment to measure the speeds of light in water. The Fizeau experiment, conducted by French physicist Hippolyte Fizeau (1819–1896), was a test to determine how the motion of a medium (water) affects the speed of light propagating through it. This was not a direct measurement of the absolute speed of light in stationary water (that had been approximated earlier), but rather an investigation into the relative speeds of light traveling with and against the flow of moving water.[30]
- **1965**: Angular momentum theory applied to optical fields, foundational for BS symmetries.[58]
- **1966**: Density operators for coherent fields at BS, enabling statistical analysis.[56]
- **1981**: General properties of lossless BS in interferometry.[48]
- **1987**: Experimental observation of HOM effect, demonstrating two-photon bunching and quantum interference.[34]
- **1989**: SU(2) symmetry and photon statistics for lossless BS.[49]
- **1995**: Unitary quantum description of BS.[57]
- **2001**: KLM protocol for efficient quantum computation with linear optics, establishing scalability using beam splitters, single-photon sources, and detectors.[36][27]
- **2002**: Demonstration that nonclassical inputs are required for BS-generated entanglement.[50]
- **2008**: Silica-on-silicon waveguide quantum circuits, advancing integrated photonic implementations of BS.[45]
- **2018–2020**: Theoretical models of frequency-dependent effects in waveguide BS, including fluctuations in HOM detection.[54][55]
- **2020–2021**: Quantum entanglement and reflection coefficients in coupled waveguide BS models; frequency-dependent theory for waveguide BS.[47][51][52]
- **2022**: Quantum entanglement for monochromatic and non-monochromatic photons on waveguide BS; comprehensive review systematizing conventional vs. frequency-dependent BS.[53]

This timeline highlights the historical development from foundational quantum formulas to the recognition of frequency-dependent effects in waveguide implementations, which are important for scalable quantum technologies.

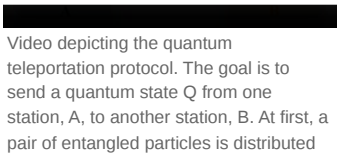

Video depicting the quantum teleportation protocol. The goal is to send a quantum state Q from one station, A, to another station, B. At first, a pair of entangled particles is distributed to A and B, which pair is shown as two particles connected by a wavy line and produced by source S. Once this preparation step is finished, the quantum teleportation itself begins. Station A measures its entangled particle together with the particle in state Q and obtains one of four possible results. These results are represented by different positions of an arrow in a "clock". The result is communicated to station B via the classical channel, represented as "radio waves". Based on the received message, station B chooses an appropriate device and applies it to its particle. In the video, the specific result measured by A is represented by an arrow pointing to the bottom right corner and so station B applies the bottom-right device. After the particle leaves the device, its state is Q, which is equal to the original state of the particle at station A. This way, the quantum teleportation of state Q is successfully completed.

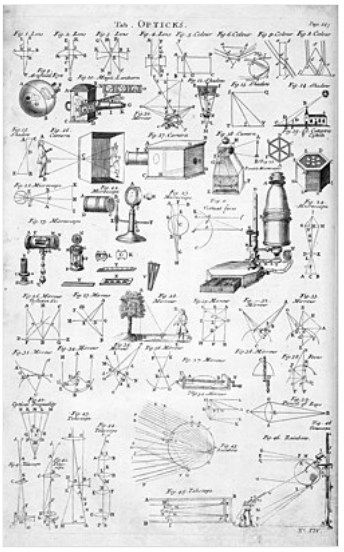

1728 Cyclopeadia. Drawings of optical equipment

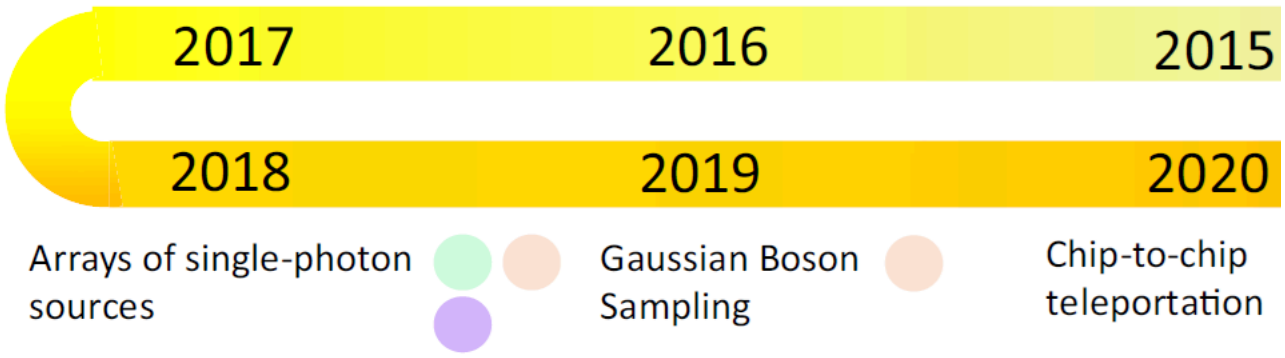

	SoS	
Operating wavelength	400-1550 nm	4(
3D capability	●	
Integration of sources	●	
Integration of detectors	●	
Coupling with fibers	●	

Integration technologies. Summary of t
what concerns the operating wavelengths, circuit
interface with external fibers. Each method is lab
achievements of quantum integrated photonics
manufacturing technology, Silica-on-Silicon (So
(Si) and silicon nitride (SiN)

$$\begin{pmatrix} \hat{b}_1 \\ \hat{b}_2 \end{pmatrix} = U_{\mathrm{BS}} \begin{pmatrix} \hat{a}_1 \\ \hat{a}_2 \end{pmatrix},$$

where the unitary matrix is given by

$$U_{\mathrm{BS}} = \begin{pmatrix} \sqrt{T}\, e^{i\phi} & \sqrt{R} \\ -\sqrt{R}\, e^{-i\phi} & \sqrt{T} \end{pmatrix}.$$

In these expressions, T, R, and ϕ represent the transmission coefficient, reflection coefficient, and relative phase, respectively. The unitary nature of U_{BS} guarantees that bosonic commutation relations are preserved.

In the angular-momentum representation, the action of the beam splitter corresponds to an SU(2) rotation generated by angular momentum operators $\hat{L}_i$. The associated rotation angles are determined by the reflectivity R and the phase ϕ.

For non-monochromatic light, the spectral degrees of freedom must also be taken into account. In this case, the output quantum state depends on the joint spectral amplitude function $\varphi(\omega_1, \omega_2)$, which must be integrated over the relevant frequency variables.

Frequency-dependent beam splitters, commonly encountered in waveguide couplers, can be derived using coupled-mode theory. Within this framework, both the reflection coefficient R and the phase ϕ depend explicitly on the frequencies ω_1 and ω_2. A representative expression for the reflection coefficient is

$$R = \sin^2\left(\frac{\Omega\, t_{\mathrm{BS}}}{2\sqrt{1+\varepsilon^2}}\right) (1+\varepsilon^2),$$

where

$$\varepsilon = \frac{\omega_2 - \omega_1}{\Omega},$$

Ω characterizes the coupling strength between the modes, and t_{BS} denotes the effective interaction time.

This spectral dependence significantly influences quantum interference and entanglement properties. To observe genuinely quantum effects, non-classical input states such as Fock states or squeezed states are required. Measures of entanglement, including concurrence, decrease when the spectral overlap between modes is limited.

Photon-number statistics also depend on both the input state and the spectral structure. Coherent states exhibit Poissonian statistics, whereas non-classical states can display sub-Poissonian or super-Poissonian behavior. In multimode fields, frequency selectivity can lead to partial photon bunching.

A prominent example of such interference phenomena is the Hong–Ou–Mandel (HOM) effect, in which two identical photons incident on a beam splitter tend to bunch together, resulting in suppressed coincidence counts. When the beam splitter is frequency dependent, spectral variations reduce the visibility of the Hong–Ou–Mandel dip. Generalizations of this effect include formulations based on wave packets as well as analogous interference phenomena involving fermions.

The beam splitter

Dates to classical interferometry in the 19th century (e.g., Michelson interferometer). Quantum applications emerged mid-20th century with quantum electrodynamics and lasers, The Hong-Ou-Mandel effect first demonstrated in 1987[34] [82][85][90]. Entanglement by a beam splitter (2002) [50] . Quantum entanglement and reflection coefficient for coupled harmonic oscillators (2020)[51]. Quantum entanglement and statistics of photons on a beam splitter in the form of coupled waveguides (2022) [52].
Beam Splitters (BS) have a variety of forms, such as a glass plate with a coat of silver or a thin dielectric film, a glass prism with a coat along its diagonal, two parallel glass plates with a coat in between, or a thin film with a deposited coat. Waveguide BSs are formed by bringing two waveguides side by side so that their electromagnetic fields interact with each other[36].

Beam splitters vary by design and frequency dependence.[61][62]

Waveguide BS (directional couplers):
Evanescent coupling between waveguides, $R(\omega) = \sin^2(\kappa(\omega)L)$.[68][69][70][71][72][73][74]

Waveguide BS:
enable integration in photonic chips for quantum technologies.[75][76][77]

Conventional beam splitters:
Cube, plate, or pellicle BS with nearly constant R, T, φ over bandwidths. Used in free-space experiments.[63][64][65][66][67]

Frequency-dependent beam splitters:
Coupled-mode theory: $d\hat{a}_1/dz = -i\,\delta\,\hat{a}_1 - i\,\kappa\,\hat{a}_2$, yielding frequency-dependent $U_{ij}(\omega)$.[91][47][52][53]

$$\begin{pmatrix} a_{\text{out},1} \\ \hat{a}_{\text{out},2} \end{pmatrix} = \begin{pmatrix} R(\omega) & T(\omega) \\ -T^*(\omega) & R(\omega) \end{pmatrix} \begin{pmatrix} a_{\text{in},1} \\ \hat{a}_{\text{in},2} \end{pmatrix}$$

Here, the reflection $R(\omega)$ and transmission $T(\omega)$ coefficients are determined by the coupling constant and the interaction length within the waveguide. This frequency dependence is crucial for accurately describing the interference of non-monochromatic single photons. [53]

Waveguide BS

Has some important advantages over a conventional BS: they are significantly more compact and have other advantages in terms of performance and integration[45]. BS can be classified in different ways, including their characteristics, such as polarizing BS and non-polarizing BS, and other distinct characteristics[48]. A BS in quantum optics can be described regardless of its physical implementation, as shown in Figure 1(a); BS illustrations vary based on BS type, as in Figure 1(b)[33]. In quantum optics, aluminium-coated beam splitters Figure 1(c) [29] are often modeled as ideal two-port devices characterized solely by R R, T T, and a relative phase shift ϕ ϕ between reflected and transmitted fields. The metallic coating introduces a well-defined phase relation between the output modes, allowing such beam splitters to be used in interference experiments, including Hong–Ou–Mandel–type configurations, despite their intrinsic losses.

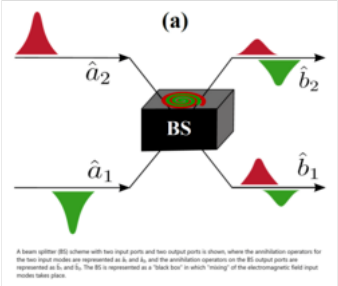

A Beam Splitter (BS) scheme with two input ports and two output ports

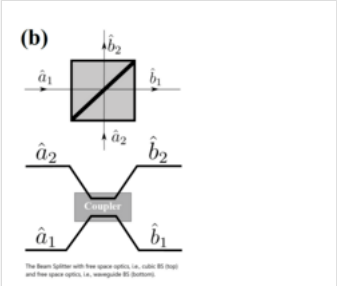

The BS with free space optics, i.e., cubic BS (top) and fiber optics, i.e., waveguide BS (bottom).

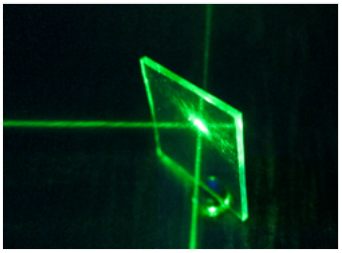

Figure 1(c). Aluminium-coated beam splitter.

Two main parameters characterizing a BS in quantum optics are the reflection coefficient R (or transmission coefficient T, which satisfies $R+T=1$) and the phase angle ϕ[49]. In conventional reviews of quantum optics, during calculations concerning the behavior of photons (or electromagnetic waves) in the output ports or in devices incorporating a BS, parameters R and ϕ are considered to be definite numbers[37].

For instance, in the Hong–Ou–Mandel (HOM) effect, an equal splitter with $R=T=\frac{1}{2}$ is used, which is independent of ϕ[34]. R and ϕ are functions of the wavelength or frequency of the incoming light, and $R=R(\lambda)$ and $\phi=\phi(\lambda)$ in both cases, regardless of which BS is used[47]. If a fixed wavelength or a small frequency band is used in the experiment, this dependency can be ignored, and the output photons can be considered constant. This has long been considered self-evident[37].

However, in some cases, R and ϕ are not constant by definition, and their frequency dependence is strong enough to affect, in a substantial way, the quantum state of light waves distributed in the output ports. Phenomena related to entanglement of light waves in a BS, unlike in the constant-parameter setting, behave differently if waveguide BSs (further referred to as fiber-optic BSs) are considered, since they differ from other BSs in this respect[47][52].

There is a theoretical basis for frequency-dependent waveguide BS. It shows that for a waveguide model interpreted as two coupled waveguides, the amplitude reflection and transmission coefficients R and T become frequency-dependent for the photons entering the BS[47]. Accounting for this frequency dependence requires corrections to established theories, such as HOM interferometer fringe analysis[54][55] and BS-generated entanglement of photons[52][53]. This pronounced frequency dependence of R and T is a distinct characteristic of waveguide BSs[47].

There is a need for a comprehensive analysis that classifies BS in quantum optics into two types: conventional (frequency-independent) and frequency-dependent. Based on this classification, researchers can examine differences in photon entanglement at the output ports. The present analysis performs exactly this, considering entanglement, photon statistics at the outputs, and the HOM effect[52][54].

Beam splitter in quantum optics

- Beam splitters also enable quantum optical neural networks for tasks like image classification and optimal quantum cloning, offering variational quantum algorithms and perceptron models that exploit entanglement for supervised learning.[282][283][284][289][290][294] Photonics-based implementations further integrate nonlinear activations and diffractive networks for all-optical machine learning.[274][275][276][280] Recent QML models address barren plateaus and demonstrate quantum verification of NP problems.[286][287][293]"

Since a beam splitter (BS) separates incoming beams, the quantum state of photons at the BS output ports is given by

$$|\text{out}\rangle = e^{i\hat{H}t_{\text{BS}}}|\text{in}\rangle,$$

where $\hat{H}$ is the Hamiltonian of the quantized electromagnetic field interacting with matter, t_{BS} is the interaction time, and $|\text{in}\rangle$ is the initial state of the electromagnetic field. $\hat{H}$ can be quite complex, depending on the type of beam splitter.

where the creation operators of the first and second modes are $\hat{a}_1$ and $\hat{a}_2$, respectively. The integers s_1 and s_2 are the quantum numbers of the first and second modes (i.e. the number of photons in each mode). The coefficients C_{s_1,s_2} define the initial state, and $|0\rangle_1|0\rangle_2$ are the vacuum states of modes 1 and 2. For convenience, it is $|0\rangle_1|0\rangle_2 \equiv |0\rangle$.

If the initial states are Fock states, then the coefficients satisfy $C_{s_1,s_2} = 1$. In this case, it is straightforward to show (up to an insignificant phase) that [31][43][56]

$$|\text{out}\rangle = \sum_{s_1,s_2} C_{s_1,s_2} \frac{1}{\sqrt{s_1! s_2!}} (\hat{b}_1^\dagger)^{s_1} (\hat{b}_2^\dagger)^{s_2} |0\rangle,$$

with

$$\hat{b}_k^\dagger = e^{i\hat{H}t_{\text{BS}}} \hat{a}_k^\dagger e^{-i\hat{H}t_{\text{BS}}}, \qquad k = 1, 2. \text{ (Eq. (2))}$$

Here $\hat{b}_1^\dagger$ and $\hat{b}_2^\dagger$ are the creation operators at the output ports of the beam splitter for modes 1 and 2, respectively.

For any lossless two-mode beam splitter, the transformation between input and output operators is governed by a unitary matrix, $\mathbf{U}_{BS}$, constrained by the conservation of energy and bosonic commutation relations:[48][49][57]

$$\begin{pmatrix} \hat{b}_1 & \hat{b}2 \end{pmatrix} = \mathbf{U}BS \begin{pmatrix} \hat{a}_1 & \hat{a}_2 \end{pmatrix} = \begin{pmatrix} t & r\, r' & t' \end{pmatrix} \begin{pmatrix} \hat{a}_1 & \hat{a}_2 \end{pmatrix} \text{ (Eq. (3)}\}$$

The requirement for unitarity ($\mathbf{U}^\dagger\mathbf{U} = \mathbf{I}$) implies that the transmission and reflection coefficients satisfy:

$|r|^2 + |t|^2 = 1$ (Energy conservation)

$r^* t' + t^* r' = 0$ (Phase relationship between ports)

For a symmetric 50:50 beam splitter, this is commonly expressed as:

$\mathbf{U}_{BS} = \frac{1}{\sqrt{2}} \begin{pmatrix} 1 & i\, i & 1 \end{pmatrix}$ In the literature, one often encounters different representations of the beam splitter matrix. The most commonly used case corresponds to a phase shift $\phi = \pi/2$, while another frequently used representation sets $\phi = 0$. In these cases the matrix U_{BS} takes the forms

$$U_{\text{BS}} = \begin{pmatrix} \sqrt{T} & i\sqrt{R} \\ i\sqrt{R} & \sqrt{T} \end{pmatrix}, \qquad U_{\text{BS}} = \begin{pmatrix} \sqrt{T} & \sqrt{R} \\ -\sqrt{R} & \sqrt{T} \end{pmatrix}. \text{ (Eq. (4)}$$

Both representations are valid only when the final result is independent of the phase shift ϕ. As shown below, many quantities of interest in quantum optics, such as quantum entanglement at the output ports of the beam splitter, do not depend on this phase. Nevertheless, using the general form given in Eq. (3).

In reality, photons are not monochromatic and their frequency distribution must be taken into account [92][96] In this case, the initial wave function of the photons is

$$|\text{in}\rangle = \sum_{s_1,s_2} C_{s_1,s_2} \frac{1}{\sqrt{s_1! s_2!}} \int \Phi(\omega_1, \omega_2) (\hat{a}_1^\dagger)^{s_1} (\hat{a}_2^\dagger)^{s_2} |0\rangle \, d\omega_1 d\omega_2, \text{ (Eq. (5))}$$

where $\Phi(\omega_1, \omega_2)$ is the joint spectral amplitude (JSA) of the two-mode wave function. Assuming normalization,

$$\int |\Phi(\omega_1, \omega_2)|^2 \, d\omega_1 d\omega_2 = 1,$$

the output state is

$$|\text{out}\rangle = \sum_{s_1,s_2} C_{s_1,s_2} \frac{1}{\sqrt{s_1! s_2!}} \int \Phi(\omega_1, \omega_2) (\hat{b}_1^\dagger)^{s_1} (\hat{b}_2^\dagger)^{s_2} |0\rangle \, d\omega_1 d\omega_2. \text{ (Eq. (6))}$$

Quantum mechanical description

The output state is $|\Psi_{out}\rangle = e^{i\hat{H}\, t_{BS}} |\Psi_{in}\rangle$, where $\hat{H}$ is the Hamiltonian and t_{BS} the interaction time.[78][79][80] For monochromatic light, the input is $|\Psi_{\text{in}}\rangle = \sum_{s_1,s_2} C_{s_1,s_2} (\hat{a}^\dagger{}_1{}^{s_1}\, \hat{a}^\dagger{}_2{}^{s_2} / \sqrt{(s_1!\, s_2!)}) |0\rangle_1 |0\rangle_2$.[81][82] The unitary matrix U_{BS} is:

$$\begin{pmatrix} \hat{b}_1 & \hat{b}_2 \end{pmatrix} = \begin{pmatrix} \sqrt{T} & e^{i\phi}\sqrt{R} & -e^{-i\phi}\sqrt{R} & \sqrt{T} \end{pmatrix} \begin{pmatrix} \hat{a}_1 & \hat{a}_2 \end{pmatrix}$$[83][84][85]

For non-monochromatic light, integrate over joint spectral amplitude $\varphi(\omega_1, \omega_2)$.[86][61][87]

Quantum entanglement

BS generates entanglement if at least one input is non-classical (e.g., squeezed or Fock state). In frequency-dependent BS, entanglement varies with spectral overlap; broadband photons may reduce concurrence.[50][51][70][71]

Quantum entanglement of photons and their statistics

As described by D.N. Makarov in 2022 [53][A]. in the Theory for the **quantum optics beam splitter**. Recent advancements in hybrid integrated circuits [146][218] have transitioned these theories from bulk optics to scalable chip-based platforms. Quantum states of light are fundamental resources for the implementation of quantum information protocols since the pioneering tests on nonlocality and quantum teleportation.[197][198] The optical device that divides an incident beam of light into two or more output beams, typically a transmitted beam and a reflected beam. In quantum optics, the quantum beam splitter is a fundamental component far beyond classical beam division: it generates quantum superposition and quantum entanglement from non-entangled inputs, reveals non-classical photon statistics, and enables key phenomena like the Hong–Ou–Mandel effect (HOM effect).[31][32][33][34][35][36] While conventional beam splitters are often bulk components, recent progress in integrated photonics [92] has allowed for on-chip implementations. For example, independent dibenzoterrylene $C_{30}H_{18}$ (DBT) molecules integrated with silicon nitride (Si_3N_4) photonic elements, a single-crystalline anthracene nanosheet doped with dibenzoterrylene (DBT) molecules[22], and gold electrodes for Stark tuning (Methods).[18][19][20][23] Waveguides have achieved stable, lifetime-limited transitions suitable for scalable quantum networks. [3] Stark tuning experiments show how 100 waveguide-coupled molecules can be tuned to the same frequency and achieve on-chip Hong–Ou–Mandel interference. The quantum theory of the beam splitter is remarkably simple, parameterized by the reflection coefficient R (or transmission T, with $R + T = 1$) and a relative phase shift φ. This minimal description underpins linear-optical quantum protocols, from interferometry to scalable computing.[37][38] Beam splitters are systematized into "conventional" (frequency-independent R and φ) and frequency-dependent types (e.g., waveguide beam splitters), with the latter affecting entanglement and interference for non-monochromatic light.[39][40][41] [42][43] [44][45] [46][47] [48][49]. This article aims at providing an exhaustive framework of the advances of integrated quantum photonic platforms, for what concerns the integration of sources, manipulation, and detectors, as well as the contributions in quantum computing, cryptography and simulations.

Photon statistics

Output distributions depend on input states and BS parameters. Coherent inputs yield coherent outputs; Fock inputs show sub/super-Poissonian statistics.[31][33][35] In frequency-dependent BS, statistics vary by mode, leading to selective bunching/antibunching.[52][51]

Hong–Ou–Mandel effect

Recent advancements have leveraged the HOM effect for quantum kernel evaluation, enabling distance computations in feature spaces for machine learning tasks.[300] This equivalence to the SWAP test further extends HOM to high-dimensional interference in spatial modes.[297][299] Classical analogs achieving 97% visibility dips confirm the role of complementarity in such systems.[298] Identical photons on 50:50 BS bunch[296], suppressing coincidence counts (HOM dip).[83][84][85][86][87]

For frequency-dependent BS, dip visibility depends on spectral overlap; fluctuations affect detection.[47][52][53][51] Generalizations: bosons/fermions, wavepackets.[88][89][90][91]

On a molecular quantum photonic chip, on-chip HOM interference was realized with a visibility of over 0.97. [4]The high visibility confirms the excellent indistinguishability of photons originating from independent sources on the same chip.Recent experiments have successfully implemented these waveguide principles on-chip. Using independent dibenzoterrylene (DBT) molecules integrated into Si_3N_4 waveguides, researchers observed on-chip quantum interference with a visibility of 0.97 ± 0.02. [3] This provides experimental proof that integrated molecular emitters can achieve the high level of indistinguishability required for scalable quantum circuits.In 2025 a novel quantum optical pattern recognition method leveraging the Hong-Ou-Mandel (HOM) effect for binary classification tasks was introduced by Simone Roncallo et all [306].This encodes input objects and trainable parameters into single-photon states, measures two-photon coincidence rates at the output of a HOM interferometer, demonstrating a superexponential resource advantage (constant $\mathcal{O}(1)$ complexity in photons and operations versus at least linear scaling in classical artificial neurons).

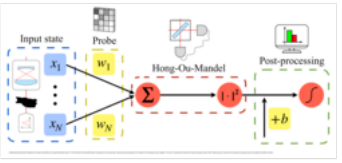

Mathematical equivalence between the Hong-Ou-Mandel and a classical artificial neuron. The left branch of the interferometer corresponds to the input layer, while the probe parameters are related to the trainable neuron weights. The rate of coincidences encodes the square absolute value of their scalar product, further post-processed by adding a bias and a sigmoid activation function

Quantum optical setup

The quantum optical setup classifies objects without reconstructing their images. The approach relies on the Hong-Ou-Mandel effect, for which the probability that two photons exit a beam splitter in different modes, depends on their distinguishability[296][297][298][299]. In the implementation, an input object is targeted by a single-photon source, and eventually followed by an arbitrary lens system. The single-photon state interferes with another one, which encodes a set of trainable parameters, e.g. through a spatial light modulator. After the Hong-Ou-Mandel interferometer, the photons are collected by two bucket detectors without spatial sensitivity, one for each output mode. Classification occurs by measuring the rate of two-photon coincidences at the output.

The Hong-Ou-Mandel effect has been successfully applied to quantum kernel evaluation[300], which can compute distances between pairs of data points in the feature space. In this case, each point is sent to one branch of the interferometer, encoded in the temporal modes of a single-photon state. In our method, the interferometer has only one independent branch, which takes the spatial modes of a single-photon state reflected off the target object. The other branch remains fixed after training, and contains the layer of parameters.[292][305] After the measurement, the response function of our apparatus mathematically resembles that

by leveraging classical implementations that bypass hardware in all the optical way. Quantum mechanical effects, like superposition and entanglement, can provide a significant speedup in such tasks[281][282], e.g. by building quantum analogues of the perceptron[283][284][285], by employing variational methods[286][287] or quantum-inspired approaches[288]. Quantum optical neural networks harness the best of both worlds, i.e. deep learning capabilities from quantum optics[289][290][291][292][293][294][295].

Mathematical description

Two optical input modes *a* and *b* that carry annihilation and creation operators $\hat{a}$, $\hat{a}^\dagger$, and $\hat{b}$, $\hat{b}^\dagger$. Identical photons in different modes can be described by the Fock states[33], so, for example $|0\rangle_a$ corresponds to mode *a* empty (the vacuum state), and inserting one photon into *a* corresponds to $|1\rangle_a = \hat{a}^\dagger|0\rangle_a$, etc. A photon in each input mode is therefore

$$|1,1\rangle_{ab} = \hat{a}^\dagger \hat{b}^\dagger |0,0\rangle_{ab}.$$

When the two modes *a* and *b* are mixed in a 1:1 beam splitter, they produce output modes *c* and *d*. Inserting a photon in *a* produces a superposition state of the outputs: if the beam splitter is 50:50 then the probabilities of each output are equal, i.e. $\hat{a}^\dagger|0\rangle_a \to \frac{1}{\sqrt{2}}\left(\hat{c}^\dagger + \hat{d}^\dagger\right)|00\rangle_{cd}$, and similarly for inserting a photon in *b*. Therefore

$$\hat{a}^\dagger \to \frac{\hat{c}^\dagger + \hat{d}^\dagger}{\sqrt{2}} \quad \text{and} \quad \hat{b}^\dagger \to \frac{\hat{c}^\dagger - \hat{d}^\dagger}{\sqrt{2}}.$$

The relative minus sign appears because the classical lossless beam splitter produces a unitary transformation[49]. This can be seen most clearly when wr the two-mode beam splitter transformation in matrix form:

$$\begin{pmatrix} \hat{a} \\ \hat{b} \end{pmatrix} \to \frac{1}{\sqrt{2}} \begin{pmatrix} 1 & 1 \\ 1 & -1 \end{pmatrix} \begin{pmatrix} \hat{c} \\ \hat{d} \end{pmatrix}.$$[48]

Similar transformations hold for the creation operators. Unitarity of the transformation implies unitarity of the matrix. Physically, this beam splitter transformation means that reflection from one surface induces a relative phase shift of π, corresponding to a factor of −1, with respect to reflection from the other side of the beam splitter (see the Physical description above)[57].

When two photons enter the beam splitter, one on each side, the state of the two modes becomes

$$\begin{aligned} |1,1\rangle_{ab} = \hat{a}^\dagger \hat{b}^\dagger |0,0\rangle_{ab} &\to \frac{1}{2}\left(\hat{c}^\dagger + \hat{d}^\dagger\right)\left(\hat{c}^\dagger - \hat{d}^\dagger\right)|0,0\rangle_{cd} \\ = \frac{1}{2}\left(\hat{c}^{\dagger 2} - \hat{d}^{\dagger 2}\right)|0,0\rangle_{cd} &= \frac{|2,0\rangle_{cd} - |0,2\rangle_{cd}}{\sqrt{2}}, \end{aligned}$$

where used $\hat{c}^{\dagger 2}|0,0\rangle_{cd} = \hat{c}^\dagger|1,0\rangle_{cd} = \sqrt{2}|2,0\rangle_{cd}$ etc.[34] Since the commutator of the two creation operators $\hat{c}^\dagger$ and $\hat{d}^\dagger$ is zero because they operate on different spaces, the product term vanishes. The surviving terms in the superposition are only the $\hat{c}^{\dagger 2}$ and $\hat{d}^{\dagger 2}$ terms. Therefore, when two identical photons enter a 1:1 beam splitter, they will always exit the beam splitter in the same (but random) output mode.

The result is non-classical: a classical light wave entering a classical beam splitter with the same transfer matrix would always exit in arm *c* due to destructive interference in arm *d*, whereas the quantum result is random. Changing the beam splitter phases can change the classical result to arm *d* or a mixture of both, but the quantum result is independent of these phases.

For a more general treatment of the beam splitter with arbitrary reflection/transmission coefficients, and arbitrary numbers of input photons, see the general quantum mechanical treatment of a beamsplitter for the resulting output Fock state.[31][32][35]

Single-Photon Detection in Beam Splitter Experiments

In experiments in quantum optics with beam splitters, an individual-photon-catching detector network is obviously decisive to glimpse those striking non-classical effects: antibunching, Hong-Ou-Mandel interference, and entanglement that the beam splitter itself can generate.

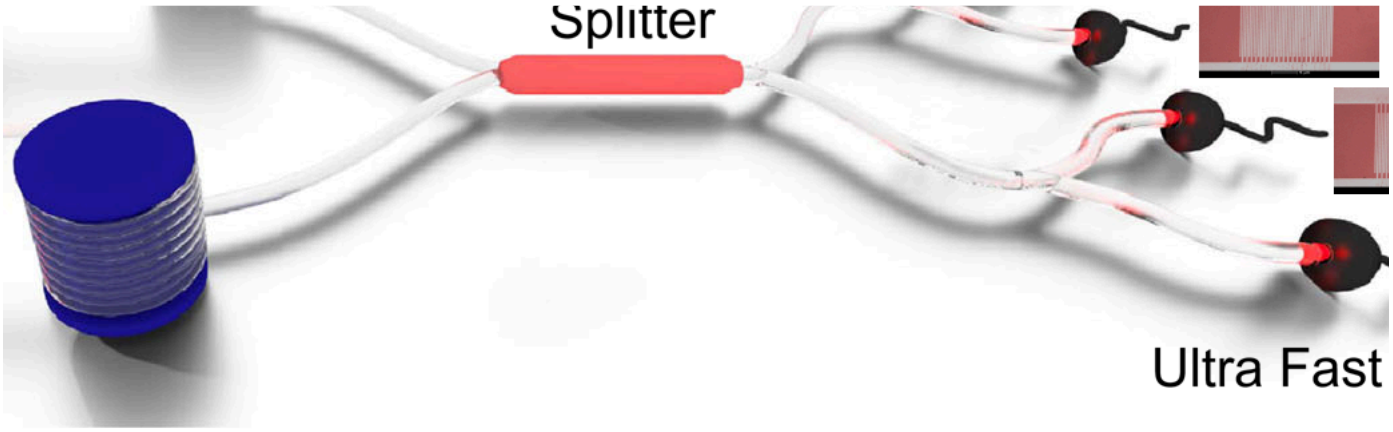

Single-photon detectors (SPDs), such as superconducting nanowire single-photon detectors (SNSPDs) or single-photon avalanche diodes (SPADs) operated in Geiger mode, provide the necessary time-resolved, high-efficiency detection at the single-photon level.[197][259][260] In foundational experiments, SPDs are placed at the two output ports of a beam splitter. For a single photon incident on 50:50 beam splitter, the absence of simultaneous detections (zero coincidence counts above vacuum noise) demonstrates the particle-like indivisibility of the photon, while interference effects reveal its wave nature (e.g., in Mach-Zehnder configurations built with beam splitters).[34][64]

In the Hong–Ou–Mandel effect, two indistinguishable photons entering separate input ports bunch at the outputs, leading to a near-complete suppression of coincidence detections between SPDs at the two ports, a hallmark of quantum interference.[34][79][80] In tests of photon statistics or entanglement generation, post-selected coincidence measurements between SPDs enable quantification of antibunching ($g^{(2)}(0) < 1$) or violation of Bell inequalities.[50][64]

Fully integrating SPDs onto photonic chips are still a big challenge. There are some promising developments about waveguide-coupled superconducting detectors. These latest developments open up the possibility that future quantum systems will have detection totally on a chip.[45][145][211] Such integrations facilitate advanced HOM-based classifiers, where SLMs encode trainable parameters for pattern recognition, with software tools enabling simulation and optimization.[302][303][304][306] Training challenges, including initialization and convergence, mirror those in deep neural networks.[301][305]

Key technologies for quantum photonic chips

Photonic integration provides a clear route toward compact quantum communication systems with growing complexity and improved functionality. Integrated quantum communication can be broadly categorized into three main aspects: photonic material platforms enabling large-scale integration[117][118][119], quantum photonic components such as quantum light sources[120], high-speed modulators[121] and highly efficient photodetectors[122], and representative applications including QKD[123][124] and quantum teleportation[125]. Because the materials, fabrication processes, and structural designs used in photonic integration differ substantially from those of discrete optical systems, essential chip-level photonic components must be redesigned and optimized for specific quantum information tasks.

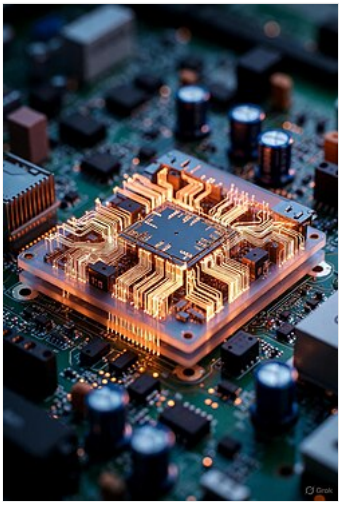

Artistic illustration of glowing optical waveguides in a silicon nitride quantum photonic integrated circuit, highlighting on-chip light propagation for quantum interference experiments.

This section summarizes key technical developments covering quantum light sources, encoding and decoding elements, quantum detectors, and packaging techniques for integrated photonic systems. These advances constitute critical points in the evolution of integrated quantum communication. Early work in this area can be traced to the integration of photon sources based on periodically poled lithium niobate waveguides[126] and interferometric circuits realized using silica-on-silicon planar lightwave circuits (PLCs)[127][128][129][130]. The high efficiency and thermally stable operation of these integrated devices highlighted their intrinsic advantages over discrete and bulky optical components.

Subsequently, a wide range of material platforms was explored, leading to substantial progress in the on-chip generation, manipulation, and detection of quantum states of light for quantum communication and other quantum information applications. Prominent monolithic platforms for chip-based quantum communication include silica waveguides (silica-on-silicon and laser-written silica waveguides), silicon-on-insulator (SOI), silicon nitride (Si_3N_4), lithium niobate (LN), gallium arsenide (GaAs)[252][255][256][17], indium phosphide (InP), and silicon oxynitride (SiO_xN_y)[115][116][131]. The state of the art of these platforms reveals distinct advantages and limitations in terms of waveguiding performance, availability of active components, and compatibility with related technologies.

SOI offers high refractive-index contrast for dense integration, strong optical nonlinearity for nonclassical state generation, and excellent compatibility with advanced CMOS (complementary metal–oxide–semiconductor) fabrication processes widely used in the semiconductor industry. However, the absence of native lasing capability complicates the full monolithic integration of all components required for a complete quantum communication system. Semiconductor

(SNSPDs)[132] and on-chip lasers for weak coherent pulse generation[133]. Additional important technologies, including semiconductor quantum dots (QDs) coupled to photonic nanostructures[133] and diamond-on-insulator platforms[134][135], have also emerged as competitive solutions for integrated quantum communication systems.

A timeline of advances in quantum photonic chips for quantum communication highlights several key items, including the first on-chip quantum interferometer for quantum cryptography[127], quantum teleportation[5][255][21] realized on a photonic chip[139], chip-based DV-QKD[123], CV-QKD[124], and MDI-QKD[138][142][143], as well as chip-to-chip quantum teleportation[125].

Encoding schemes:

Path encoding

Photon states distributed among multiple waveguides are employed to encode qubit/qudit states and to observe quantum interference effects due to bosonic statistics. Such information encoding has been one of the most investigated in quantum integrated photonics. Path-encoded single- and multi-photon states can be arbitrarily prepared, manipulated and measured using re-programmable Mach–Zehnder interferometers (MZIs). The effect of the MZI is equivalent to the operations made by a beamsplitter with a tunable splitting ratio and by a phase shift (Fig. 3a). This unit for path encoding processing envisages two unbiased directional couplers and two integrated tunable phase shifts. Relative phases between paths in integrated devices are the results of the geometric deformation of waveguides. The recent developments in the field have demonstrated the capability to realize reconfigurable phase shifters, thus allowing the implementation of several unitary transformations on the same device [206][213][254]. There are several examples of programmable integrated devices in SoS[206][220] , Si [208] [210] [215] [248] [249] [251], SiN[207][209][254] silica laser written waveguides with FLW[241] [242] [243] and UV-writing[221][222]. The re-programmable elements inside the MZI are the two phase shifts that are controlled generally through the thermo-optic effect. Heaters placed nearby the location of the waveguide allow for local changes in the refractive index of the material. Such reconfigurable units are sufficient to encode, process and measure any qubit in two optical paths. The complexity reached from integrated devices is nowadays very remarkable allowing for full integration of qubit- and qudit-based quantum gates and algorithms in SoS [220] and Si-chips [210][215][250][251]. In particular, the most recent silicon quantum processors count up to 16 integrated single-photon sources, more than 100 heaters and likewise integrated optical elements[208][210][215].

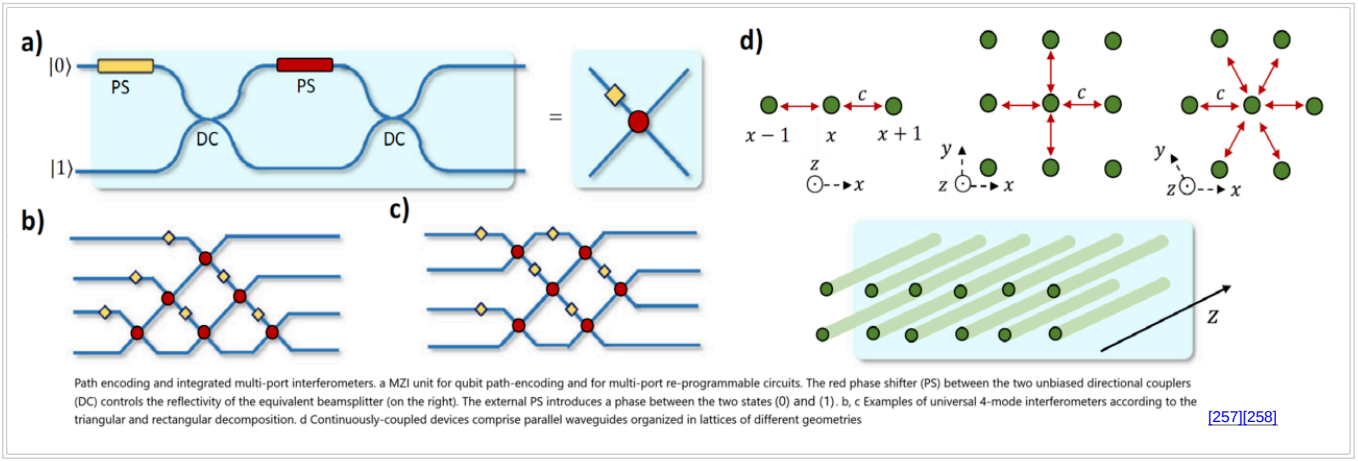

Path encoding and integrated multi-port interferometers. a MZI unit for qubit path-encoding and for multi-port re-programmable circuits. The red phase shifter (PS) between the two unbiased directional couplers (DC) controls the reflectivity of the equivalent beamsplitter (on the right). The external PS introduces a phase between the two states (0) and (1). b, c Examples of universal 4-mode interferometers according to the triangular and rectangular decomposition. d Continuously-coupled devices comprise parallel waveguides organized in lattices of different geometries [257][258]

Femtosecond-laser-writing (FLW)

The femtosecond laser writing, using Mode locking[28] is a further method for silica waveguide fabrication[217][223]. The mechanism of the process is the non-linear absorption of strong laser pulses tightly focused in the silica sample. Such absorption results in a permanent and localized modification in the refractive index. Waveguides are directly written by translating the silica sample at a constant speed with respect to the laser beam, without needing any preliminary preparation of substrate or layers of different materials as in the previous methods. The cross-section is circular and presents a very low birefringence. Such characteristics together with the 3D geometry capability have allowed the realization of devices insensitive from polarization [224][226] as well as devices able to manipulate polarization as waveplates or partially polarizing beamsplitter [227][228]. The 3D geometry has other advantages regarding the range of possible schemes for optical circuit decomposition. FLW devices demonstrated to realize circuits according to the traditional networks of integrated beam-splitter in planar [225][229][230][231][232] and 3D geometries[233][234][235] and continuously coupled waveguide lattices [236][237][238][239][240]. There are instances of re-programmable circuits in small[241][242][243][244] and large scale [245] realization of integrated devices. The integration of single-photon sources exploiting nonlinear effects is still challenging due to the low birefringence ($\Delta n \approx 0$) and the null third-order nonlinear susceptibility ($\chi^{(3)} = 0$) of these waveguides. Notwithstanding, femtosecond laser writing (FLW) can be exploited to write waveguides in a nonlinear material to generate pairs of photons through parametric processes. These kinds of sources have been interfaced successfully with FLW chips in[246]. The FLW waveguides display also a good coupling with external fibers, enabling the interface of the optical circuit with remote users or solid-state sources[243][244].

Compact integration of optical components

A factor that drives the compact integration of optical components, quantum computing on integrated photonic chips has attracted much attention in recent years. There are two types of optical models[163]: specific quantum computing models[164][165] (e.g., boson sampling), and universal quantum computing models[166] [167][168][169][170][171] (e.g., one-way or measurement-based). For specific quantum computation, a variety of photonic systems were demonstrated using quantum photonic chips[172][173][174][175][176][177][177][179], enabling a natural and effective implementation of boson sampling. Gaussian boson

heralding version[141][166], and compiled Shor's factorization[165]. Moreover, both architectural and technological efforts have been dedicated to photonic one-way quantum computation. This approach employs cluster states and sequential single-qubit measurement to perform universal quantum algorithms[167][169][190] and can be greatly enhanced by implementing resource state generation and fusion operation natively[191][192][193]. The relevant circuit implementations include programmable fourphoton graph states on a Si chip[194], path-polarization hyperentangled and cluster states on a SiO_2 chip[195] and programmable eight-qubit graph states on a Si chip[196]. In conclusion, quantum photonic chips have rapidly matured to become a versatile platform that proves to be invaluable in the development of cutting-edge quantum communication technologies. This review delves into the advancements achieved in this particular field. Considering the remarkable outcomes, it is anticipated that photonic integration will eventually assume a crucial role in building various quantum networks and potentially a global quantum internet[112][113][114][16], reshaping the landscape of future communication methodologies.

Chip packaging and system integration

While bare quantum photonic chips can be characterized using a probe station, they must be packaged into durable modules to develop working prototype devices[147]. To this end, numerous processes have been proposed to package quantum photonic chips into compact systems for real-world applications. Generally, photonic packaging involves a range of techniques and technical competencies needed to make the optical, electrical, mechanical, and thermal connections between a photonic chip and the off-chip components in a photonic module[148][149][150]. Fiber-to-chip coupling is one of the best-known aspects. The main challenge associated with coupling between an optical fiber and a typical waveguide on the chip is the large difference between their mode-field diameters (MFDs)[151]. For example, the MFD at 1550 nm is ~10 μm in telecom single-mode fiber (SMF), while the cross-section of the corresponding strip silicon waveguide is usually only 220 × 450 nm. This mismatch can be mitigated by using configurations that efficiently extract the mode from waveguide[144], such as inverted-taper edge couplers interfaced with lensed SMF fibers[152][153] or ultrahigh numerical aperture fibers[154], and grating couplers interfaced with SMF fibers[151][155]. For the approach harnessing grating couplers, coupling efficiency up to 81.3% (−0.9 dB) can be achieved in a 260-nm-thick SOI platform without the need for a back reflector or overlayer[156]. Additionally, efficiencies over 90% have been experimentally demonstrated using edge couplers fabricated on 200-mm SOI wafers[157]. An alternative approach for cost-effective and panel-level packaging is the evanescent coupling scheme, which has been reported to have a coupling loss of approximately 1 dB at a wavelength of 1550 nm[158]. To access the electrical components on quantum photonic chips, electronic packaging is required to route signals from electronic drivers, amplifiers, and other control circuitry. This is often achieved by interfacing with dedicated printed circuit boards (PCBs)[159]. The connection between PCBs and the bond-pads on the chip is usually made using wire-bonds.When a very large number of electrical connections or precise sub-nanosecond control on multiple channels is needed, 2.5-dimensional or 3-dimensional integration with customized electronic integrated circuits (EICs) may be utilized [147][160] This integration can be achieved using either solder-ballbump or copper-pillar-bump interconnects, providing a robust electrical, mechanical, and thermal interface for the photonic chips[161][162]. Global thermal stabilization of quantumphotonic devices is essential for prototypes that require high accuracy and repeatability or for field tests where seasonal temperature swings are common. This can be achieved using passive cooling techniques or a thermoelectric cooler (TEC). The added global stability from the TEC allows for more efficient and better reproducibility in the local temperature tuning of individual photonic elements (e.g., micro-ring resonators, thermo-optic phase shifters, etc.) on the chip[147]. Additionally, liquid cooling can be installed to further increase the cooling capacity of the system[159]

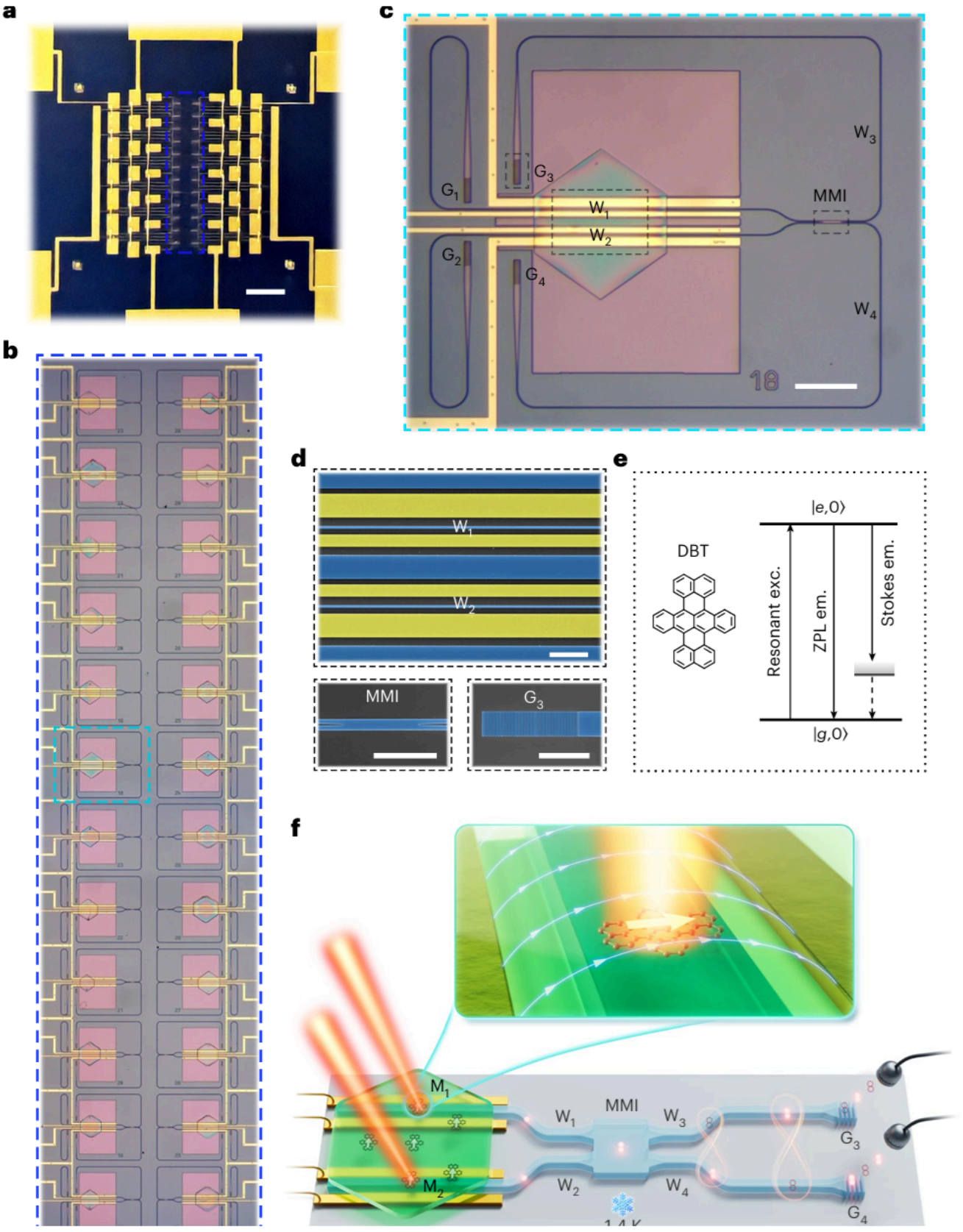

Molecular quantum photonic chip and an illustration of on-chip interference of indistinguishable single photons from independent quantum emitters (molecules).

and one of the output gratings G3. **e**, DBT molecular structure and energy-level scheme. em., emission; exc., excitation. **f**, Illustration of the on-chip two-photon quantum interference experiment: two streams of single photons

implemented these waveguide principles using molecular quantum photonic chips. By integrating independent dibenzoterrylene (DBT) molecules into Si_3N_4 waveguides, researchers have achieved on-chip Hong–Ou–Mandel (HOM) interference with a visibility of 0.97 ± 0.02. [3]

These integrated systems allow for the observation of quantum beating when a frequency detuning (e.g., 400 MHz) is applied between two emitters. These beats have been shown to persist for over 100 μs, demonstrating the high spectral stability and single-photon purity required for scalable quantum information processing. [2]

Evaluating photon indistinguishability from the TPQI experiment under CW excitation

A recent report[24] establishes a method to evaluate full wave-packet photon indistinguishability from TPQI experiments under non-resonant CW excitation. Here, this method extends to resonant CW excitation, enabling direct assessment of photon indistinguishability from our TPQI data. The metric used in this approach is $\tilde{V}(S) = \frac{\int d\tau \left[1 - g^{(2)}_{\mathrm{HOM}}(\tau)\right] - \int d\tau \left[1 - g^{(2)}_{\mathrm{HOM},d}(\tau)\right]}{\int d\tau \left[1 - g^{(2)}_{\mathrm{HOM},d}(\tau)\right]}$.

Substituting the theoretical expressions for $g^{(2)}_{\mathrm{HOM}}(\tau)$ and $g^{(2)}_{\mathrm{HOM},d}(\tau)$ from equations respectively,

$\tilde{V}(S)$ is

$$\tilde{V}(S) = \frac{\mathcal{M}(2\mathcal{M}+1)}{\mathcal{M} + (\mathcal{M}+1)/(1+S)}.$$

where $\mathcal{M} = \frac{\tau_2}{2\tau_1}$. Equation (26) expresses $\tilde{V}$ as a function of S.

In the weak excitation limit ($S \to 0$), $\tilde{V}$ reduces to $\frac{\tau_2}{2\tau_1}$, thereby yieldingn the true photon indistinguishability, consistent with TPQI experiments under pulsed excitation[24].

Applications

Image classification

Has been significantly improved by the introduction of deep learning methods, which provide several algorithms that can learn and extract image features. Examples include feedforward neural networks, convolutional neural networks and vision transformers[268][269][270][271]. The artificial neuron, also called perceptron[272], represents the fundamental unit of such architectures. In this model, encoded data are processed through a set of weighted trainable connections, by taking the scalar product between the input and the vector of weights. The output is further post-processed, including a bias and an activation function, which is usually non-linear[273]. Image classification implies a two-fold cost. Computational processing requires a number of operations that scales, at least, linearly in the image resolution. Similarly, the optical cost of image capturing undergoes the same scaling in the number of photons.

This model compared against conventional classifiers, i.e. a single neuron and a convolutional neural network, commonly employed in pattern recognition tasks[292][293][294][295][305]. Adopting the TensorFlow notation, the convolutional structure is: Conv2D (10, 3 × 3) → Conv2D (4, 2 × 2) → MaxPooling2D (2 × 2). Roughly, all the architectures have ~10^3 trainable parameters. The performances are equal in the MNIST dataset, both in terms of trainability and final accuracy. In the CIFAR-10 dataset, our classifier outperforms the conventional ones, showing superior efficiency under a strongly-constrained parameters count. These findings emphasize the competitive accuracy of our method, and also its comparative advantage in pattern recognition tasks with a limited number of parameters.

Entanglement distribution and quantum teleportation systems

Quantum teleportation has been achieved over different types of platforms such as superconducting qubits, trapped atoms, nitrogen-vacancy centers, and continuous-variable states, among others.[261] Of all the types of quantum teleportation, the photonic qubit is considered to be a very promising candidate for forming the quantum channel of the quantum network due to its stability within noisy environments and the fact that it can be operated at room temperature.[214] Photonic qubits[1] are more resistant to long-distance environmental interference. To date, photonic quantum teleportation has been successfully performed experimentally using different methods, including free-space and fiber.[261]

The first experimental validation of quantum teleportation relied on qubits encoded in the polarization of photons produced from a beta-barium borate (BBO) crystal in a free-space setup on an optical table.[212] Later, the distance record for free-space teleportation was pushed beyond 1,400 km between the Micius satellite and a ground station,[262] thus providing the basis for a global quantum network. However, due to the issues of beam divergence, pointing, and collection of free-space teleportation, optical-fiber-based teleportation is considered more suitable for the establishment of cost-efficient quantum metropolitan networks. The current distance record for optical-fiber-based teleportation is 102 km.[263]

A major issue related to photonic qubit teleportation involves the efficiency limit of Bell-state measurements (BSMs) using linear optics, with a 50% bound. To go around such a constraint, continuous variable optical modes can be used as a different solution to accomplish full deterministic teleportation. This technique was successfully experimented with on a 6-km fiber link,[264] but its fidelity needs to be enhanced because of its vulnerability to transmission losses. For non-

chip, including path-encoded entanglement in Mach-Zehnder Interferometers (MZIs),[250] polarization entanglement created in birefringent media,[266] and time-bin entanglement in Franson interferometers.[267]

The first telecom-based chip-scale teleportation used an off-chip photon source, showing the feasibility of a fidelity of 0.89 in a single chip system.[248] The current advancement in integrated quantum photonics has also helped realize entanglement-based quantum communications beyond the chip level. The first entanglement distribution between chips incorporated all necessary components into monolithically integrated silicon photonic chips.[253] On-chip entangled Bell states were generated, and the qubit was transferred to the other silicon chip by encoding the on-chip path-encoded and in-fiber polarization states using two-dimensional grating couplers. Moreover, more advanced integrated quantum circuits implemented with on-chip sources have implemented inter-chip teleportation, showing a fidelity of 0.88.[216] The chip-scale realization of photonic qubit creation, processing, and transmission provides one potential promising step toward the realization of the distributed quantum information processing Internet. In addition, entangled photon pairs in the visible and telecom bands have been created on a chip of silicon nitride (Si_3N_4) using a micro-ring resonator, with distribution over more than 20 km, using precisely designed and fabricated micro-ring resonators, entangling photons in the visible range, which can be coupled with quantum memories, and in the telecom range, with lower attenuation in the transmission of the photons over the fibers.[229]

Quantum Information Processing and Computing

Beam splitters are the fundamental building blocks for Linear Optical Quantum Computing (LOQC).

- The KLM Protocol: Beam splitters facilitate the probabilistic entangling gates necessary for universal quantum computation using only linear elements. The original CNOT gate in this protocol operates with a success probability of $\frac{1}{16}$. [27]
- Waveguide Lattices: Integrated arrays of beam splitters allow for the simulation of quantum walks and complex multi-photon interference patterns. [45][46]

Quantum Photonic Chips for Quantum Communication and Internet

The smallest optical beam splitters are typically found in advanced research within nanophotonics, plasmonics, and integrated optics[115], where devices are miniaturized for applications like photonic computing[39], optical communications, and quantum technologies[46]. These are far smaller than commercial or conventional beam splitters (which often measure millimeters to centimeters)[59].

Photonic Beam Splitters

An example is a silicon-based photonic polarizing beam splitter developed by researchers at the University of Utah. It measures just 2.4 × 2.4 microns (μm) in footprint, making it one of the smallest low-loss all-dielectric designs[47]. This device splits incoming light into two separate polarized channels and was designed to enable light-speed computing by replacing electrons with photons[36]. It was published in 2015 and claimed as the world's smallest at the time.[48]

Plasmonic Beam Splitters

Plasmonic designs, which use surface plasmon polaritons (waves at metal-dielectric interfaces) to manipulate light, can be even smaller due to sub-wavelength confinement, though they often have higher losses[60]. One ultracompact plasmonic polarizing beam splitter on a silicon-on-insulator (SOI) platform has a coupling region of 1.1 μm in length and 50 nanometers (nm) in width. The overall footprint is approximately 1.1 × 0.95 μm (accounting for the waveguides), resulting in an area of about 1 μm². This was reported in 2013 and leverages silver cylinders sandwiched between silicon waveguides for splitting polarized light.[137] Other plasmonic variants, such as those based on nanoslits or bent directional couplers, have dimensions ranging from hundreds of nm to a few μm, with some coupling lengths as short as 0.9–8.9 μm in more recent designs (e.g., from 2020–2023 papers on slot waveguides or photonic crystals).[116]

Metasurface-Based Beam Splitters

Metasurfaces (ultra-thin engineered arrays of nano-antennas) offer nanoscale thickness, often 50–200 nm, while lateral dimensions can be a few μm to tens of μm to handle the beam. These are among the thinnest possible, enabling flat optics for beam splitting with arbitrary ratios or angles[79]. A 2018 example uses gradient metasurfaces for nanoscale thickness, though specific lateral sizes vary by design (typically 5–10 μm across for efficient operation).[133]

These nanoscale beam splitters are fabricated using techniques like electron-beam lithography and are integrated on chips[106], making them orders of magnitude smaller than traditional glass cubes or plates[29]. Recent developments (post-2020) focus on reducing losses, broadening bandwidth, and integrating with materials like lithium niobate or silicon nitride[136], but no widely reported designs have broken below ~1 μm in key dimensions while maintaining functionality[49]. If you're interested in a specific type (e.g., for visible light, IR, or quantum applications), more details could narrow it down further[57].

Quantum communication

which applies the principles of quantum mechanics for quantum information transmission, enables fundamental improvements to security, computing, sensing, and metrology. This realm encapsulates a vast variety of technologies and applications ranging from state-of-the-art laboratory experiments to commercial reality. The best-known example is quantum key distribution (QKD)[92][93]. The basic idea of QKD is to use the quantum states of photons to share secret keys between two distant parties. The quantum no-cloning theorem endows the two communicating users with the ability to detect any eavesdropper trying to gain knowledge of the key[94][95]. Since security is based on the laws of quantum physics rather than computational complexity, QKD is recognized as a desired solution to address the ever-increasing threat raised by emergent quantum computing hardware and algorithms.

authentication and long-term security of keys[109].

Quantum Communication and Cryptography

Beam splitters are used to distribute entanglement across networks, enabling secure information transfer.

- Quantum Key Distribution (QKD): Critical for implementing protocols that detect eavesdropping through signal splitting and interference. [61][62]
- Quantum Repeaters: Used in Bell-state measurements (BSM) to perform entanglement swapping, extending the range of quantum communication. [78]
- Teleportation: A beam splitter is used to perform the joint measurement required to transfer a quantum state $|\psi\rangle$ between distant nodes. [65][66]

Quantum Metrology and Sensing

By creating path-entangled states, such as N00N states of the form $(|N,0\rangle + |0,N\rangle)/\sqrt{2}$, beam splitters allow sensors to surpass the Standard Quantum Limit.

- Heisenberg-Limit Sensing: Utilizing quantum interference to achieve a phase sensitivity $\Delta\phi$ that scales with $1/N$ rather than the classical $1/\sqrt{N}$. [75][76][77]
- Beam splitter interference in HOM setups enhances metrological precision in quantum kernel methods for feature space analysis.[291][300]

Characterization and Foundations

To verify the performance of these applications, measures and tests are employed:

- Entanglement Measures: The quality of the generated states is quantified using Concurrence and Entropy of Formation. [72][73]
- Foundational Tests: Beam splitters provide the platform for Bell test violations and studies of decoherence in open quantum systems. [63][64]

Integrated Photonics

Implementations focusing at on-chip integration using waveguide architectures. An improvement is the use of dibenzoterrylene (DBT) molecules in an anthracene matrix, which has enabled the on-chip integration of independent channels with high-visibility, indistinguishable single photons. [25]

See also

- Hong–Ou–Mandel effect
- Waveguide (optics)
- Integrated quantum photonics
- Linear optical quantum computing

- Quantum
- Quantum A Matter Of Size
- Quantum A Spooky Action at a Distance
- Quantum: A Walk Through the Universe
- Number of independent spatial modes in a spherical volume
- Quantum Computing Algorithms in the NISQ Era
- Quantum Formulas Collection
- Quantum Matter Elements and Particles
- Quantum mechanics
- Quantum mechanics/Timeline
- Quantum mechanics measurements
- Quantum Noisy Qubits
- Quantum optics beam splitter experiments
- Quantum: The Secret of Cohesion: How Waves Hold Matter Together
- Quantum Ultra fast lasers
- Template:Quantum optics operators
- Physical Sciences

Sources

- Theory for the beam splitter in quantum optics: quantum entanglement of photons and their statistics, HOM effect. 2022 (https://arxiv.org/pdf/2211.03359)
  This reference provides a comprehensive theoretical framework for conventional and frequency-dependent beam splitters. It systematizes how the reflection coefficient and phase shift impact quantum entanglement and photon statistics at the output ports.
- Recent progress in quantum photonic chips for quantum communication and internet 2023 (https://www.nature.com/articles/s41377-023-01173-8)
  A review of the state-of-the-art in integrated quantum photonics, focusing on the development of chip-scale components for quantum communication networks and the challenges of multi-photon interference.
- Integrated photonics in quantum technologies 2023 (https://link.springer.com/article/10.1007/s40766-023-00040-x)
  This paper explores the transition from bulk optics to integrated circuits, highlighting how waveguide-based miniaturization is essential for scaling quantum technologies
- On-chip quantum interference of indistinguishable single photons from integrated independent molecules. (https://ngdc.cncb.ac.cn/openlb/publication/OLB-PM-41193863)
  This study demonstrates a molecular quantum photonic chip using dibenzoterrylene (DBT) molecules. By integrating these into organic nanosheets and Si_3N_4 waveguides, stable transitions are achieved. This approach builds on the fundamental principles of waveguide-coupled emitters and quantum networks.
- Quantum optical classifier with superexponential speedup 2025 (https://www.nature.com/articles/s42005-025-02020-5)
  This paper introduces a quantum optical pattern recognition method for binary classification using the Hong-Ou-Mandel effect in a beam splitter-based interferometer. It achieves superexponential speedup by classifying objects without image reconstruction, requiring constant $\mathcal{O}(1)$ resources in photons and operations, providing an advantage over classical neurons.

🎯 Primary Learning Objective

After working through this resource, students should be able to:

- Define a beam splitter and explain its role in quantum optics.
- Mathematically describe how a beam splitter transforms quantum modes.
- Understand and analyze key experiments, especially the Hong–Ou–Mandel (HOM) effect.
- Connect beam splitter behavior to fundamental quantum concepts such as superposition and entanglement.
- Relate modern integrated photonics implementations (e.g., waveguide beam splitters) to traditional optics.

Rev. Mod. Phys. **79**: 135–174. doi:10.1103/RevModPhys.79.135.
2. Qiang, X. G.; et al. (2018). "Large-scale silicon quantum photonics implementing arbitrary two-qubit processing". *Nat. Photon.* **12**: 534–539. doi:10.1038/s41566-018-0236-y.
3. Pelucchi, E.; et al. (2022). "The potential and global outlook of integrated photonics for quantum technologies". *Nat. Rev. Phys.* **4**: 194–208. doi:10.1038/s42254-021-00398-z.
4. Lodahl, P.; Mahmoodian, S.; Stobbe, S. (2015). "Interfacing single photons and single quantum dots with photonic nanostructures". *Rev. Mod. Phys.* **87**: 347–400. doi:10.1103/RevModPhys.87.347.
5. Llewellyn, D.; et al. (2020). "Chip-to-chip quantum teleportation and multi-photon entanglement in silicon". *Nat. Phys.* **16**: 148. doi:10.1038/s41567-019-0727-x.
6. He, Y. M.; et al. (2013). "On-demand semiconductor single-photon source with near-unity indistinguishability". *Nat. Nanotechnol.* **8**: 213–217. doi:10.1038/nnano.2012.262.
7. Somaschi, N. et al. Near-optimal single-photon sources in the solid state. *Nat. Photon.* **10**, 340–345 (2016). https://doi.org/10.1038/nphoton.2016.23
8. Rezai, M.; Wrachtrup, J.; Gerhardt, I. Coherence properties of molecular single photons for quantum networks. *Phys. Rev. X* **8**, 031026 (2018). https://doi.org/10.1103/PhysRevX.8.031026
9. Liu, F. et al. High Purcell factor generation of indistinguishable on-chip single photons. *Nat. Nanotechnol.* **13**, 835–840 (2018). https://doi.org/10.1038/s41565-018-0188-x
10. Evans, R. E. et al. Photon-mediated interactions between quantum emitters in a diamond nanocavity. *Science* **362**, 662 (2018). https://doi.org/10.1126/science.aau4691
11. Wan, N. H. et al. Large-scale integration of artificial atoms in hybrid photonic circuits. *Nature* **583**, 226–231 (2020). https://doi.org/10.1038/s41586-020-2441-3
12. Chen, D. et al. Quantum interference of resonance fluorescence from germanium-vacancy color centers in diamond. *Nano Lett.* **22**, 6306–6312 (2022). https://doi.org/10.1021/acs.nanolett.2c01959
13. Martínez, J. A. et al. Photonic indistinguishability of the tin-vacancy center in nanostructured diamond. *Phys. Rev. Lett.* **129**, 173603 (2022). https://doi.org/10.1103/PhysRevLett.129.173603
14. Türschmann, P. et al. Chip-based all-optical control of single molecules coherently coupled to a nanoguide. *Nano Lett.* **17**, 4941–4945 (2017). https://doi.org/10.1021/acs.nanolett.7b02033
15. Toninelli, C. et al. Single organic molecules for photonic quantum technologies. *Nat. Mater.* **20**, 1615–1628 (2021). https://doi.org/10.1038/s41563-021-00987-4
17. Liu, J. et al. Single self-assembled InAs/GaAs quantum dots in photonic nanostructures: the role of nanofabrication. *Phys. Rev. Appl.* **9**, 064019 (2018). https://doi.org/10.1103/PhysRevApplied.9.064019
18. Zhai, L. et al. Quantum interference of identical photons from remote GaAs quantum dots. *Nat. Nanotechnol.* **17**, 829–833 (2022). https://doi.org/10.1038/s41565-022-01131-2
19. Lettow, R. et al. Quantum interference of tunably indistinguishable photons from remote organic molecules. *Phys. Rev. Lett.* **104**, 123605 (2010). https://doi.org/10.1103/PhysRevLett.104.123605
20. Papon, C.; et al. (2023). "Independent operation of two waveguide-integrated quantum emitters". *Phys. Rev. Appl.* **19**: L061003. doi:10.1103/PhysRevApplied.19.L061003.
21. Gao, W. B.; et al. (2013). "Quantum teleportation from a propagating photon to a solid-state spin qubit". *Nat. Commun.* **4**: 2744. doi:10.1038/ncomms3744.
22. Nicolet, A. A.; et al. (2007). "Single dibenzoterrylene molecules in an anthracene crystal: main insertion sites". *ChemPhysChem* **8**: 1929–1936. doi:10.1002/cphc.200700340.
23. Proux, R.; et al. (2015). "Measuring the photon coalescence time window in the continuous-wave regime for resonantly driven semiconductor quantum dots". *Phys. Rev. Lett.* **114**: 067401. doi:10.1103/PhysRevLett.114.067401.
24. Schofield, R. C.; et al. (2022). "Photon indistinguishability measurements under pulsed and continuous excitation". *Phys. Rev. Res.* **4**: 013037. doi:10.1103/PhysRevResearch.4.013037.
25. Lange, Christian M.; et al. (2025). "Cavity QED with molecular defects coupled to a photonic crystal cavity". arXiv:2506.01917.
26. Huang, T.; Xu, M.; Jin, W.; Liu, W.; Chi, Y.; Tang, J.; Ren, P.; Wei, S. *et al*. (2025). "On-chip quantum interference of indistinguishable single photons from integrated independent molecules". *Nature Nanotechnology*. doi:10.1038/s41565-025-02043-7.
27. Myers, Anne; Laflamme, Raymond (2003). "Linear Optics Quantum Computation: An Overview". arXiv:quant-ph/0305082.
28. Mayer, B.; et al. (2017). "Long-term mutual phase locking of picosecond pulse pairs generated by a semiconductor nanowire laser". *Nature Communications* **8**: 15521. https://www.nature.com/articles/ncomms15521.
29. Macleod, H. A. (2018). "Thin-Film Optical Filters" (5th ed.). Boca Raton: CRC Press / Taylor & Francis. doi:10.1201/b21960. ISBN 9781351982238.
31. Mandel, L.; Wolf, E. (1995). "Optical Coherence and Quantum Optics". Cambridge: Cambridge University Press. ISBN 9780521417112.
32. Scully, M.; Zubairy, M. (1997). "Quantum Optics". Cambridge: Cambridge University Press. doi:10.1017/CBO9780511813993.
33. Rodney Loudon (2000). "The Quantum Theory of Light". Oxford University Press. doi:10.1093/oso/9780198501770.002.0001. ISBN 9780198501770.
34. Hong, C. K.; Ou, Z. Y.; Mandel, L. (1987). "Measurement of subpicosecond time intervals between two photons by interference". *Physical Review Letters* **59** (18): 2044–2046. doi:10.1103/PhysRevLett.59.2044. PMID 10035403.
35. Agarwal, G. S. (2013). "Quantum Optics". Cambridge: Cambridge University Press. ISBN 9781107006409.
36. Knill, E.; Laflamme, R.; Milburn, G. J. (2001). "A scheme for efficient quantum computation with linear optics". *Nature* **409**: 46–52. doi:10.1038/35051009.
37. Pan, J. W. (2012). "Multiphoton entanglement and interferometry". *Rev. Mod. Phys.* **84**: 777. doi:10.1103/RevModPhys.84.777.
38. Sangouard, N.; Simon, C.; de Riedmatten, H.; Gisin, N. (2011). "Quantum repeaters based on atomic ensembles and linear optics". *Rev. Mod. Phys.* **83**: 33. doi:10.1103/RevModPhys.83.33.
39. Nicholas, C. H. (2017). "Quantum transport simulations in a programmable nanophotonic processor". *Nature Photonics* **11**: 447–452. doi:10.1038/nphoton.2017.95.
40. Tambasco, J.-L. (2018). "Quantum interference of topological states of light". *Sci Adv.* **4**: eaat3187. doi:10.1126/sciadv.aat3187.
41. Pezze, L.; Smerzi, A.; Oberthaler, M. K.; Schmied, R.; Treutlein, P. (2018). "Quantum metrology with nonclassical states of atomic ensembles". *Rev. Mod. Phys.* **90**: 035005. doi:10.1103/RevModPhys.90.035005.
42. Weedbrook, C. (2012). "Gaussian quantum information". *Rev. Mod. Phys.* **84**: 621. doi:10.1103/RevModPhys.84.621.
43. Ou, Z.-Y. J. (2007). "Multi-Photon Quantum Interference". New York: Springer. doi:10.1007/978-0-387-25554-5.
44. Bromberg, Y.; Lahini, Y.; Morandotti, R.; Silberberg, Y. (2009). "Quantum and classical correlations in waveguide lattices". *Phys. Rev. Lett.* **102**: 253904. doi:10.1103/PhysRevLett.102.253904.

resurgence of the linear optics quantum interferometer– recent advances and applications". *Reviews in Physics* **4**: 100030. doi:10.1016/j.revip.2019.100030.

47. Makarov, D. N. (2021). "Theory of a frequency-dependent beam splitter in the form of coupled waveguides". *Scientific Reports* **11**: 5014. doi:10.1038/s41598-021-84588-w.
48. Zeilinger, A. (1981). "General properties of lossless beam splitters in interferometry". *American Journal of Physics* **49**: 882. doi:10.1119/1.12387.
49. Campos, R. A.; Saleh, B. E. A.; Teich, M. C. (1989). "Quantum-mechanical lossless beam splitter: Su(2) symmetry and photon statistics". *Phys. Rev. A* **40**: 1371. doi:10.1103/PhysRevA.40.1371.
50. Kim, M. S.; Son, W.; Buzek, V.; Knight, P. L. (2002). "Entanglement by a beam splitter: Nonclassicality as a prerequisite for entanglement". *Phys. Rev. A* **65**: 032323. doi:10.1103/PhysRevA.65.032323.
51. Makarov, D. (2020). "Quantum entanglement and reflection coefficient for coupled harmonic oscillators". *Physical Review E* **102**: 052213. doi:10.1103/PhysRevE.102.052213.
52. Makarov, D.; et al. (2021). "Quantum entanglement and statistics of photons on a beam splitter in the form of coupled waveguides". *Scientific Reports* **11**: 10274. doi:10.1038/s41598-021-89838-5.
53. Makarov, D.; Tsykareva, Y. (2022). "Quantum entanglement of monochromatic and non-monochromatic photons on a waveguide beam splitter". *Entropy* **24**: 49. doi:10.3390/e24010049.
54. Makarov, D. N. (2020). "Theory of hom interference on coupled waveguides". *Optics Letters* **45**: 6322–6325. doi:10.1364/OL.410518.
55. Makarov, D. N. (2020). "Fluctuations in the detection of the hom effect". *Scientific Reports* **10**: 20124. doi:10.1038/s41598-020-77189-6.
56. Titulaer, U.; Glauber, R. (1966). "Density operators for coherent fields". *Phys. Rev.* **145**: 1041. doi:10.1103/PhysRev.145.1041.
57. Luis, A.; Sánchez-Soto, L. (1995). "A quantum description of the beam splitter". *Quantum Semiclass. Opt.* **7**: 153–160. doi:10.1088/1355-5111/7/2/005.
58. Biedenharn, L. C.; van Dam, H. (1965). "Quantum Theory of Angular Momentum". Academic Press. ISBN 9781114824430.
59. Thorlabs 50:50 (R:T) non-polarizing beamsplitter cube. Example product: BS005, 700-1100 nm. Manufacturer page: https://www.thorlabs.com/thorproduct.cfm?partnumber=BS005.
60. Huang, W.-P. (1994). "Coupled-mode theory for optical waveguides: an overview". *J. Opt. Soc. Am. A* **11**: 963–983. doi:10.1364/JOSAA.11.000963.
61. Ekert, A. (1991). "Quantum cryptography based on Bell's theorem". *Phys. Rev. Lett.* **67**: 661. doi:10.1103/PhysRevLett.67.661.

decoherence in quantum computer memory". *Phys. Rev. A* **52**: R2493. doi:10.1103/PhysRevA.52.R2493.

64. Aspect, A.; Grangier, P.; Roger, G. (1981). "Experimental tests of realistic local theories via Bell's theorem". *Phys. Rev. Lett.* **47**: 460–463. doi:10.1103/PhysRevLett.47.460.
65. Samuel, L.; Braunstein, H.; Kimble, J. (1998). "Teleportation of continuous quantum variables". *Phys. Rev. Lett.* **80**: 869–872. doi:10.1103/PhysRevLett.80.869.
66. Ekert, A.; Knight, P. (1995). "Entangled quantum systems and the Schmidt decomposition". *Amer. J. Phys.* **63**: 415–423. doi:10.1119/1.17904.
67. Grobe, R.; Rzazewski, K.; Eberly, J. (1994). "Measure of electron-electron correlation in atomic physics". *J. Phys. B* **27**: L503–L508. doi:10.1088/0953-4075/27/16/001.
68. Bennett, C.; Bernstein, H.; Popescu, S.; Schumacher, B. (1996). "Concentrating partial entanglement by local operations". *Phys. Rev. A* **53**: 2046–2052. doi:10.1103/PhysRevA.53.2046.
69. Casini, H.; Huerta, M. (2009). "Entanglement entropy in free quantum field theory". *J. Phys. A: Math. Theor.* **42**: 504007. doi:10.1088/1751-8113/42/50/504007.
70. Chen, Y.; Hsieh, M. (2021). "Quantum entanglement by a beam splitter analogous to laser mode transformation by a cylindrical lens". *Optics Letters* **46**: 5129–5132. doi:10.1364/OL.437609.
71. Jiang, Z.; Lang, M.; Caves, C. (2013). "Mixing nonclassical pure states in a linear-optical network almost always generates modal entanglement". *Phys. Rev. A* **88**: 044301. doi:10.1103/PhysRevA.88.044301.
72. Berrada, K.; Baz, M. E.; Saif, F.; Hassouni, Y.; Mnia, S. (2009). "Entanglement generation from deformed spin coherent states using a beam splitter". *J. Phys. A: Math. Theor.* **42**: 285306. doi:10.1088/1751-8113/42/28/285306.
73. Xiang-bin, W. (2002). "Theorem for the beam-splitter entangler". *Phys. Rev. A* **66**: 024303. doi:10.1103/PhysRevA.66.024303.
74. Makarov, D. N. (2017). "High intensity generation of entangled photons in a two-mode electromagnetic field". *Annalen der Physik* **549**: 1600408. doi:10.1002/andp.201600408.
75. Holland, M.; Burnett, K. (1993). "Interferometric detection of optical phase shifts at the Heisenberg limit". *Phys. Rev. Lett.* **71**: 1355. doi:10.1103/PhysRevLett.71.1355.
76. Polino, E.; Valeri, M.; Spagnolo, N.; Sciarrino, F. (2020). "Photonic quantum metrology". *AVS Quantum Science* **2**: 024703. doi:10.1116/5.0007577.
77. Phoenix, S.; Knight, P. (1988). "Fluctuations and entropy in models of quantum optical resonance". *Annals of Physics* **186**: 381–407. doi:10.1016/0003-4916(88)90006-1.

Am. B **6**: 917–927. doi:10.1364/JOSAB.6.000917.

80. Steinberg, A.; Kwiat, P.; Chiao, R. Y. (1992). "Dispersion cancellation and high-resolution time measurements in a fourth-order optical interferometer". *Phys. Rev. A* **45**: 6659. doi:10.1103/PhysRevA.45.6659.
81. Legero, T.; Wilk, T.; Hennrich, M.; Rempe, G.; Kuhn, A. (2004). "Quantum beat of two single photons". *Phys. Rev. Lett.* **93**: 070503. doi:10.1103/PhysRevLett.93.070503.
82. Lyons, A. (2018). "Attosecond-resolution Hong–Ou–Mandel interferometry". *Phys. Rev. Lett.* **4**: 9416. doi:10.1126/sciadv.aap9416.
83. Wang, K. (2006). "Quantum theory of two-photon wavepacket interference in a beamsplitter". *J. Phys. B: At. Mol. Opt. Phys.* **39**: R293. doi:10.1088/0953-4075/39/23/R01.
84. Branczyk, A. M. (2017). "Hong–Ou–Mandel interference". arXiv:1711.00080.
85. Lim, Y.; Beige, A. (2005). "Generalized Hong–Ou–Mandel experiments with bosons and fermions". *New J. Phys.* **7**: 155. doi:10.1088/1367-2630/7/1/155.
86. Toyoda, K.; Hiji, R.; Noguchi, A.; Urabe, S. (2015). "Quantum theory of two-photon wavepacket interference in a beamsplitter". *Nature* **527**: 74–77. doi:10.1038/nature15521.
87. Aspect, A. (2019). "Hanbury Brown and Twiss, Hong Ou and Mandel effects and other landmarks in quantum optics: from photons to atoms". Oxford University Press. doi:10.1093/oso/9780198837190.003.0012.
88. Grice, W.; Walmsley, I. (1997). "Spectral information and distinguishability in type-II down-conversion with a broadband pump". *Phys. Rev. A* **56**: 1627. doi:10.1103/PhysRevA.56.1627.
89. Erdmann, R.; Branning, D.; Grice, W.; Walmsley, I. A. (2000). "Restoring dispersion cancellation for entangled photons produced by ultrashort pulses". *Phys. Rev. A* **62**: 053810. doi:10.1103/PhysRevA.62.053810.
90. Barbieri, M.; et al. (2017). "What Hong–Ou–Mandel interference says on two-photon frequency entanglement". *Sci. Rep.* **7**: 7247. doi:10.1038/s41598-017-07555-4.
91. Shih, Y. (1999). "Advances in Atomic, Molecular, and Optical Physics". Cambridge: Academic Press. ISBN 9780120038411.
92. Bennett, C. H.; Brassard, G.Flamini (1984). *Quantum cryptography: Public key distribution and coin tossing*. International Conference on Computers, Systems and Signal Processing. Bangalore, India: IEEE. pp. 175–179.
93. Bennett, C. H.; Bessette, F.; Brassard, G.; Salvail, L.; Smolin, J. (1992). "Experimental quantum cryptography". *J. Cryptol.* **5** (1): 3–28. doi:10.1007/BF00191318.

H. (2002). "Quantum cryptography". *Rev. Mod. Phys.* **74** (1): 145–195. doi:10.1103/RevModPhys.74.145.

96. Xu, F. H.; Ma, X.; Zhang, Q.; Lo, H.-K.; Pan, J.-W. (2020). "Secure quantum key distribution with realistic devices". *Rev. Mod. Phys.* **92** (2). doi:10.1103/RevModPhys.92.025002.
97. Wang, S.; Yin, Z.-Q.; He, D.-Y. (2022). "Twin-field quantum key distribution over 830-km fibre". *Nat. Photonics* **16** (2): 154–161. doi:10.1038/s41566-021-00928-2.
98. Chen, Y.-A.; Zhang, Q.; Chen, T.-Y. (2021). "An integrated space-to-ground quantum communication network over 4,600 kilometres". *Nature* **589** (7841): 214–219. doi:10.1038/s41586-020-03093-8.
99. Li, W.; Zhang, L.; Tan, H. (2023). "High-rate quantum key distribution exceeding 110 Mb s–1". *Nat. Photonics* **17** (5): 416–421. doi:10.1038/s41566-023-01166-4.
100. Peev, M. (2009). "The SECOQC quantum key distribution network in Vienna". *N. J. Phys.* **11** (7). doi:10.1088/1367-2630/11/7/075001.
101. Stucki, D. (2011). "Long-term performance of the SwissQuantum quantum key distribution network in a field environment". *N. J. Phys.* **13** (12). doi:10.1088/1367-2630/13/12/123001.
102. Avesani, M. (2022). "Deployment-ready quantum key distribution over a classical network infrastructure in Padua". *J. Lightwave Technol.* **40**: 1658–1663. doi:10.1109/JLT.2021.3130447.
103. Sasaki, M. (2011). "Field test of quantum key distribution in the Tokyo QKD network". *Opt. Express* **19**: 10387–10409. doi:10.1364/OE.19.010387.
104. Chen, T. Y. (2009). "Field test of a practical secure communication network with decoy-state quantum cryptography". *Opt. Express* **17**: 6540–6549. doi:10.1364/OE.17.006540.
105. Wang, S. (2014). "Field and long-term demonstration of a wide area quantum key distribution network". *Opt. Express* **22**: 21739–21756. doi:10.1364/OE.22.021739.
106. Dynes, J. F. (2019). "Cambridge quantum network". *npj Quantum Inf.* **5**. doi:10.1038/s41534-019-0231-5.
107. Scarani, V. (2009). "The security of practical quantum key distribution". *Rev. Mod. Phys.* **81**: 1301–1350. doi:10.1103/RevModPhys.81.1301.
108. Diamanti, E. (2016). "Practical challenges in quantum key distribution". *npj Quantum Inf.* **2**. doi:10.1038/npjqi.2016.25.
109. Wang, L. J. (2021). "Experimental authentication of quantum key distribution with post-quantum cryptography". *npj Quantum Inf.* **7**. doi:10.1038/s41534-021-00409-2.
110. Bouwmeester, D. (1997). "Experimental quantum teleportation". *Nature* **390**: 575–579. doi:10.1038/37539.
111. Furusawa, A.; Sørensen, J. L.; Braunstein, S. L. (1998). "Unconditional quantum teleportation". *Science* **282**: 706–709. doi:10.1126/science.282.5389.706.

doi:10.1038/nature07127.

114. Long, G. L.; Pan, D. (2022). "An evolutionary pathway for the quantum internet relying on secure classical repeaters". *IEEE Netw.* **36**: 82–88. doi:10.1109/MNET.108.2100375.
115. Orieux, A.; Diamanti, E. (2016). "Recent advances on integrated quantum communications". *J. Opt.* **18**.
116. Wang, J. W. (2020). "Integrated photonic quantum technologies". *Nat. Photonics* **14**: 273–284. doi:10.1038/s41566-020-0619-8.
117. Matthews, J. C. F. (2009). "Manipulation of multiphoton entanglement in waveguide quantum circuits". *Nat. Photonics* **3**: 346–350. doi:10.1038/nphoton.2009.89.
118. Siew, S. Y. (2021). "Review of silicon photonics technology and platform development". *J. Lightwave Technol.* **39**: 4374–4389. doi:10.1109/JLT.2021.3075325.
119. Smit, M.; Williams, K.; van der Tol, J. (2019). "Past, present, and future of InP-based photonic integration". *APL Photonics* **4**. doi:10.1063/1.5097179.
120. Joshi, C. (2018). "Frequency multiplexing for quasi-deterministic heralded single-photon sources". *Nat. Commun.* **9**. doi:10.1038/s41467-018-03286-5.
121. He, M. B. (2019). "High-performance hybrid silicon and lithium niobate Mach–Zehnder modulators for 100 Gbit s−1 and beyond". *Nat. Photonics* **13**: 359–364. doi:10.1038/s41566-019-0441-6.
122. Pernice, W. H. P. (2012). "High-speed and high-efficiency travelling wave single-photon detectors embedded in nanophotonic circuits". *Nat. Commun.* **3**. doi:10.1038/ncomms2328.
123. Sibson, P. (2017). "Chip-based quantum key distribution". *Nat. Commun.* **8**. doi:10.1038/ncomms13984.
124. Zhang, G. (2019). "An integrated silicon photonic chip platform for continuous-variable quantum key distribution". *Nat. Photonics* **13**: 839–842. doi:10.1038/s41566-019-0549-3.
125. Llewellyn, D. (2020). "Chip-to-chip quantum teleportation and multi-photon entanglement in silicon". *Nat. Phys.* **16**: 148–153. doi:10.1038/s41567-019-0733-2.
126. Tanzilli, S. (2002). "PPLN waveguide for quantum communication". *Eur. Phys. J. D* **18**: 155–160. doi:10.1140/epjd/e20020035.
127. Bonfrate, G. (2001). "Asymmetric Mach-Zehnder germano-silicate channel waveguide interferometers for quantum cryptography systems". *Electron. Lett.* **37**: 846–847. doi:10.1049/el:20010627.
128. Honjo, T.; Inoue, K.; Takahashi, H. (2004). "Differential-phase-shift quantum key distribution experiment with a planar light-wave circuit Mach–Zehnder interferometer". *Opt. Lett.* **29**: 2797–2799. doi:10.1364/OL.29.002797.
129. Takesue, H. (2005). "Differential phase shift quantum key distribution experiment over 105 km fibre". *N. J. Phys.* **7**. doi:10.1088/1367-2630/7/1/232.

quantum photonic circuits". *Nat. Photonics* **14**: 285–298. doi:10.1038/s41566-019-0568-0.

132. Agnesi, C.; Reimer, M. E.; Jöns, K. D. (2019). "Hong–Ou–Mandel interference between independent III–V on-silicon waveguide integrated lasers". *Opt. Lett.* **44**: 271–274. doi:10.1364/OL.44.000271.
133. Lodahl, P.; Mahmoodian, S.; Stobbe, S. (2015). "Interfacing single photons and single quantum dots with photonic nanostructures". *Rev. Mod. Phys.* **87**: 347–400. doi:10.1103/RevModPhys.87.347.
134. Schröder, T. (2016). "Quantum nanophotonics in diamond [Invited]". *J. Opt. Soc. Am. B* **33**: B65–B83. doi:10.1364/JOSAB.33.000B65.
135. Lenzini, F. (2018). "Diamond as a platform for integrated quantum photonics". *Adv. Quantum Technol.* **1**. doi:10.1002/aqt2.1800061.
136. Saravi, S.; Pertsch, T.; Setzpfandt, F. (2021). "Lithium niobate on insulator: an emerging platform for integrated quantum photonics". *Adv. Opt. Mater.* **9**. doi:10.1002/adom.202100789.
137. Ma, Y. J. (2015). "Symmetrical polarization splitter/rotator design and application in a polarization insensitive WDM receiver". *Opt. Express* **23**: 16052–16062. doi:10.1364/OE.23.016052.
138. Semenenko, H. (2020). "Chip-based measurement-device-independent quantum key distribution". *Optica* **7**: 238–242. doi:10.1364/OPTICA.7.000238.
139. Metcalf, B. J. (2014). "Quantum teleportation on a photonic chip". *Nat. Photonics* **8**: 770–774. doi:10.1038/nphoton.2014.197.
140. Wang, J. W. (2014). "Gallium arsenide (GaAs) quantum photonic waveguide circuits". *Opt. Commun.* **327**: 49–55. doi:10.1016/j.optcom.2014.03.041.
141. Carolan, J. (2015). "Universal linear optics". *Science* **349**: 711–716. doi:10.1126/science.aaa1555.
142. Wei, K. J. (2020). "High-speed measurement-device-independent quantum key distribution with integrated silicon photonics". *Phys. Rev. X* **10**. doi:10.1103/PhysRevX.10.031030.
143. Cao, L. (2020). "Chip-based measurement-device-independent quantum key distribution using integrated silicon photonic systems". *Phys. Rev. Appl.* **14**. doi:10.1103/PhysRevApplied.14.011001.
144. Marchetti, R. (2019). "Coupling strategies for silicon photonics integrated chips [Invited]". *Photonics Res.* **7**: 201–239. doi:10.1364/PRJ.7.000201.
145. Sprengers, J. P.; Gaggero, A.; Sahin, D. (2011). "Waveguide superconducting single-photon detectors for integrated quantum photonic circuits". *Appl. Phys. Lett.* **99**. doi:10.1063/1.3657518.
146. Sahin, D. (2013). "Waveguide photon-number-resolving detectors for quantum photonic integrated circuits". *Appl. Phys. Lett.* **103**. doi:10.1063/1.4820842.

review of the ePIXpack photonics packaging platform". *IEEE J. Sel. Top. Quantum Electron.* **17**: 645–651. doi:10.1109/JSTQE.2011.2161469.

149. O'Brien, P. (2016). Pavesi, L.; Lockwood, D. J. (eds.). "Packaging of silicon photonic devices". Berlin: Springer. pp. 217–236.
150. Lee, J. S. (2016). "Meeting the electrical, optical, and thermal design challenges of photonic-packaging". *IEEE J. Sel. Top. Quantum Electron.* **22**. doi:10.1109/JSTQE.2016.2562638.
151. Taillaert, D. (2006). "Grating couplers for coupling between optical fibers and nanophotonic waveguides". *Jpn. J. Appl. Phys.* **45**: 6071–6077. doi:10.1143/JJAP.45.6071.
152. Pu, M. H. (2010). "Ultra-low-loss inverted taper coupler for silicon-on-insulator ridge waveguide". *Opt. Commun.* **283**: 3678–3682. doi:10.1016/j.optcom.2010.07.005.
153. He, L. Y. (2019). "Low-loss fiber-to-chip interface for lithium niobate photonic integrated circuits". *Opt. Lett.* **44**: 2314–2317. doi:10.1364/OL.44.002314.
154. Preble, S. F. (2015). "On-chip quantum interference from a single silicon ring-resonator source". *Phys. Rev. Appl.* **4**. doi:10.1103/PhysRevApplied.4.021001.
155. Sacher, W. D. (2014). "Wide bandwidth and high coupling efficiency Si3N4-on-SOI dual-level grating coupler". *Opt. Express* **22**: 10938–10947. doi:10.1364/OE.22.010938.
156. Marchetti, R. (2017). "High-efficiency grating-couplers: demonstration of a new design strategy". *Sci. Rep.* **7**. doi:10.1038/s41598-017-16750-7.
157. Bakir, B. B. (2010). "Low-loss (<1 dB) and polarization-insensitive edge fiber couplers fabricated on". *IEEE Photonics Technol. Lett.* **22**: 739–741. doi:10.1109/LPT.2010.2061039.
158. Dangel, R. (2015). "Polymer waveguides for electro-optical integration in data centers and high-performance computers". *Opt. Express* **23**: 4736–4750. doi:10.1364/OE.23.004736.
159. Taballione, C. (2021). "A universal fully reconfigurable 12-mode quantum photonic processor". *Mater. Quantum Technol.* **1**: 035002. doi:10.1088/2633-4356/ac1a9f.
160. Abrams, N. C. (2020). "Silicon photonic 2.5D multi-chip module transceiver for high-performance data centers". *J. Lightwave Technol.* **38**: 3346–3357. doi:10.1109/JLT.2020.2979551.
161. Wörhoff, K. (2004). "Flip-chip assembly for photonic circuits". *Proceedings of SPIE*. Micro-Optics: Fabrication, Packaging, and Integration (Strasbourg, France: SPIE) **5454**: 9–20. doi:10.1117/12.544610.

Microelectronics and Microsystems. Bordeaux, France: IEEE. pp. 1–7. doi:10.1109/ESIME.2010.5464484.

163. Pelucchi, E. (2022). "The potential and global outlook of integrated photonics for quantum technologies". *Nat. Rev. Phys.* **4**: 194–208. doi:10.1038/s42254-021-00398-z.
164. Aaronson, S.; Arkhipov, A. (2011). *The computational complexity of linear optics*. Proc. 43rd Annual ACM Symposium on Theory of Computing. San Jose: ACM. pp. 333–342. doi:10.1145/1993636.1993682.
165. Rohde, P. P.; Ralph, T. C. (2012). "Error tolerance of the boson-sampling model for linear optics quantum computing". *Phys. Rev. A* **85**. doi:10.1103/PhysRevA.85.022332.
166. Knill, E.; Laflamme, R.; Milburn, G. J. (2001). "A scheme for efficient quantum computation with linear optics". *Nature* **409**: 46–52. doi:10.1038/35051009.
167. Raussendorf, R.; Briegel, H. J. (2001). "A one-way quantum computer". *Phys. Rev. Lett.* **86**: 5188–5191. doi:10.1103/PhysRevLett.86.5188.
168. Nielsen, M. A. (2004). "Optical quantum computation using cluster states". *Phys. Rev. Lett.* **93**. doi:10.1103/PhysRevLett.93.040503.
169. Walther, P. (2005). "Experimental one-way quantum computing". *Nature* **434**: 169–176. doi:10.1038/nature03347.
170. Menicucci, N. C.; Flammia, S. T.; Pfister, O. (2008). "One-way quantum computing in the optical frequency comb". *Phys. Rev. Lett.* **101**. doi:10.1103/PhysRevLett.101.130501.
171. Saggio, V. (2021). "Experimental quantum speed-up in reinforcement learning agents". *Nature* **591**: 229–233. doi:10.1038/s41586-021-03281-8.
172. Spring, J. B. (2013). "Boson sampling on a photonic chip". *Science* **339**: 798–801. doi:10.1126/science.1231692.
173. Broome, M. A. (2013). "Photonic Boson sampling in a tunable circuit". *Science* **339**: 794–798. doi:10.1126/science.1231440.
174. Tillmann, M. (2013). "Experimental boson sampling". *Nat. Photonics* **7**: 540–544. doi:10.1038/nphoton.2013.102.
175. Crespi, A. (2013). "Integrated multimode interferometers with arbitrary designs for photonic boson sampling". *Nat. Photonics* **7**: 545–549. doi:10.1038/nphoton.2013.112.
176. Bentivegna, M. (2015). "Experimental scattershot boson sampling". *Sci. Adv.* **1**. doi:10.1126/sciadv.1400255.
177. Wang, H. (2017). "High-efficiency multiphoton boson sampling". *Nat. Photonics* **11**: 361–365. doi:10.1038/nphoton.2017.63.
178. Arrazola, J. M. (2021). "Quantum circuits with many photons on a programmable nanophotonic chip". *Nature* **591**: 54–60. doi:10.1038/s41586-021-03235-0.
179. Paesani, S. (2019). "Generation and sampling of quantum states of light in a silicon chip". *Nat. Phys.* **15**: 925–929. doi:10.1038/s41567-019-0567-8.
182. Zhong, H. S. (2020). "Quantum computational advantage using photons". *Science* **370**: 1460–1463. doi:10.1126/science.abe8770.
183. Madsen, L. S. (2022). "Quantum computational advantage with a programmable photonic processor". *Nature* **606**: 75–81. doi:10.1038/s41586-022-04516-6.
184. Arrazola, J. M.; Bromley, T. R. (2018). "Using Gaussian Boson sampling to find dense subgraphs". *Phys. Rev. Lett.* **121**. doi:10.1103/PhysRevLett.121.030503.
185. Quesada, N. (2019). "Franck–Condon factors by counting perfect matchings of graphs with loops". *J. Chem. Phys.* **150**. doi:10.1063/1.5093093.
186. Banchi, L. (2020). "Molecular docking with Gaussian Boson sampling". *Sci. Adv.* **6**. doi:10.1126/sciadv.aax1950.
187. Huh, J.; Yung, M. H. (2017). "Vibronic Boson sampling: generalized Gaussian Boson sampling for molecular vibronic spectra at finite temperature". *Sci. Rep.* **7**. doi:10.1038/s41598-017-07080-2.
188. Politi, A. (2008). "Silica-on-silicon waveguide quantum circuits". *Science* **320**: 646–649. doi:10.1126/science.1155441.
189. Politi, A.; Matthews, J. C. F.; O'Brien, J. L. (2009). "Shor's quantum factoring algorithm on a photonic chip". *Science* **325**: 1221. doi:10.1126/science.1173731.
190. Bourassa, J. E. (2021). "Blueprint for a scalable photonic fault-tolerant quantum computer". *Quantum* **5**. doi:10.22331/q-2021-02-04-392.
191. Rudolph, T. (2017). "Why I am optimistic about the silicon-photonic route to quantum computing". *APL Photonics* **2**. doi:10.1063/1.4976737.
192. Browne, D. E.; Rudolph, T. (2005). "Resource-efficient linear optical quantum computation". *Phys. Rev. Lett.* **95**. doi:10.1103/PhysRevLett.95.010501.
193. Pant, M. (2019). "Percolation thresholds for photonic quantum computing". *Nat. Commun.* **10**. doi:10.1038/s41467-019-08944-1.
194. Adcock, J. C. (2019). "Programmable four-photon graph states on a silicon chip". *Nat. Commun.* **10**. doi:10.1038/s41467-019-11335-2.
195. Ciampini, M. A. (2016). "Path-polarization hyperentangled and cluster states of photons on a chip". *Light Sci. Appl.* **5**. doi:10.1038/lsa.2016.64.
196. Vigliar, C. (2021). "Error-protected qubits in a silicon photonic chip". *Nat. Phys.* **17**: 1137–1143. doi:10.1038/s41567-021-01265-5.
197. Flamini, F.; Spagnolo, N.; Sciarrino, F. (2018). "Photonic quantum information processing: a review". *Rep. Prog. Phys.* **82**. doi:10.1088/1361-6633/aad5b2.
198. Slussarenko, S.; Pryde, G. J. (2019). "Photonic quantum information processing: A concise review". *Appl. Phys. Rev.* **6** (4). doi:10.1063/1.5115814.

"Phase-programmable Gaussian boson sampling using stimulated squeezed light". *Phys. Rev. Lett.* **127**. doi:10.1103/PhysRevLett.127.180502.

201. Madsen, L. S.; Laudenbach, F.; Askarani, M. F. (2022). "Quantum computational advantage with a programmable photonic processor". *Nature* **606** (7912): 75–81. doi:10.1038/s41586-022-04725-x.
202. Liao, S.-K. (2017). "Satellite-to-ground quantum key distribution". *Nature* **549** (7670): 43–47. doi:10.1038/nature23655.
203. Ren, J.-G. (2017). "Ground-to-satellite quantum teleportation". *Nature* **549** (7670): 70–73. doi:10.1038/nature23675.
204. Wang, J.; Sciarrino, F.; Laing, A.; Thompson, M. G. (2020). "Integrated photonic quantum technologies". *Nat. Photonics* **14** (5): 273–284. doi:10.1038/s41566-019-0532-1.
205. Pelucchi, E. (2022). "The potential and global outlook of integrated photonics for quantum technologies". *Nat. Rev. Phys.* **4** (3): 194–208. doi:10.1038/s42254-021-00398-z.
206. Carolan, J. (2015). "Universal linear optics". *Science* **349** (6249): 711–716. doi:10.1126/science.aab3642.
207. Taballione, C. (2022). "20-Mode Universal Quantum Photonic Processor". arXiv:2203.01801.
208. Qiang, X. (2018). "Large-scale silicon quantum photonics implementing arbitrary two-qubit processing". *Nat. Photonics* **12** (9): 534–539. doi:10.1038/s41566-018-0236-y.
209. Arrazola, J. M. (2021). "Quantum circuits with many photons on a programmable nanophotonic chip". *Nature* **591** (7848): 54–60. doi:10.1038/s41586-021-03202-1.
210. Chi, Y. (2022). "A programmable qudit-based quantum processor". *Nat. Commun.* **13** (1). doi:10.1038/s41467-022-28767-x.
211. Ferrari, S. (2018). "Waveguide-integrated superconducting nanowire single-photon detectors". *Nanophotonics* **7** (11): 1725–1758. doi:10.1515/nanoph-2018-0059.
212. Harrow, A. W.; Montanaro, A. (2017). "Quantum computational supremacy". *Nature* **549**: 203. doi:10.1038/nature23458.
213. Nielsen, M. A.; Chuang, I. L. (2010). "Quantum Computation and Quantum Information: 10th Anniversary Edition". Cambridge: Cambridge University Press. doi:10.1017/CBO9780511976667.
214. Cozzolino, D. (2019). "High-dimensional quantum communication: Benefits, progress, and future challenges". *Adv. Quantum Technol.* **2** (12). doi:10.1002/qute.201900038.
215. Wang, J. (2018). "Multidimensional quantum entanglement with large-scale integrated optics". *Science*. doi:10.1126/science.aar7053.
216. Svalgaard, M. (1994). "Direct UV writing of buried singlemode channel waveguides in Ge-doped silica films". *Electron. Lett.* **30** (17): 1401–1403. doi:10.1049/el:19940935.

Photonic Integrated Circuits". *Laser & Photonics Rev.* **12** (4). doi:10.1002/lpor.201700256.

219. Dietrich, C. P. (2016). "GaAs integrated quantum photonics: Towards compact and multi-functional quantum photonic integrated circuits". *Laser & Photonics Rev.* **10** (6): 870–894. doi:10.1002/lpor.201500321.
220. Shadbolt, P.J. (2012). "Generating, manipulating and measuring entanglement and mixture with a reconfigurable photonic circuit". *Nat. Photonics* **6** (1): 45–49. doi:10.1038/nphoton.2011.283.
221. Metcalf, B.J. (2014). "Quantum teleportation on a photonic chip". *Nat. Photonics* **8** (10): 770–774. doi:10.1038/nphoton.2014.217.
222. Mennea, P.L. (2018). "Modular linear optical circuits". *Optica* **5** (9): 1087–1090. doi:10.1364/OPTICA.5.001087.
223. Meany, T. (2015). "Laser written circuits for quantum photonics". *Laser & Photonics Reviews* **9** (4): 363–384. doi:10.1002/lpor.201500061.
224. Sansoni, L. (2012). "Two-particle bosonic-fermionic quantum walk via integrated photonics". *Phys. Rev. Lett.* **108** (1). doi:10.1103/physrevlett.108.010502.
225. Crespi, A. (2013). "Anderson localization of entangled photons in an integrated quantum walk". *Nature Photonics* **7**: 322–328. doi:0.1038/nphoton.2013.26.
226. Pitsios, I. (2017). "Photonic simulation of entanglement growth and engineering after a spin chain quench". *Nat. Commun.* **8** (1). doi:10.1038/s41467-017-01589-y.
227. Crespi, A. (2011). "Integrated photonic quantum gates for polarization qubits". *Nat. Commun.* **2** (1). doi:10.1038/ncomms1570.
228. Corrielli, G. (2014). "Rotated waveplates in integrated waveguide optics". *Nat. Commun.* **5** (1). doi:10.1038/ncomms5249.
229. Tillmann, M. (2013). "Experimental boson sampling". *Nature Photon.* **7** (7): 540–544. doi:10.1038/nphoton.2013.102.
230. Crespi, A. (2013). "Integrated multimode interferometers with arbitrary designs for photonic boson sampling". *Nature Photon.* **7** (7): 545–548. doi:10.1038/nphoton.2013.112.
231. Bentivegna, M. (2015). "Experimental scattershot boson sampling". *Sci. Adv.* **1** (3). doi:10.1126/sciadv.1400255.
232. Tillmann, M. (2015). "Generalized multiphoton quantum interference". *Phys. Rev. X* **5**. doi:10.1103/PhysRevX.5.041015.
233. Spagnolo, N. (2013). "Threephoton bosonic coalescence in an integrated tritter". *Nature Commun.* **4**. doi:10.1038/ncomms2616.
234. Crespi, A. (2016). "Suppression law of quantum states in a 3d photonic fast fourier transform chip". *Nat. Commun.* **7** (1). doi:10.1038/ncomms10469.
235. Viggianiello, N. (2018). "Experimental generalized quantum suppression law in sylvester interferometers". *New J. Phys.* **20** (3). doi:10.1088/1367-2630/aaad92.

quantum walks in optical lattices". *Science* **347** (6227): 1229–1233. doi:10.1126/science.1260364.

238. Caruso, F. (2016). "Fast escape of a quantum walker from an integrated photonic maze". *Nat. Commun.* **7**. doi:10.1038/ncomms11682.
239. Jiao, Z.-Q. (2020). "Two-Dimensional Quantum Walk of Correlated Photons". *arXiv*. doi:abs/2007.06554.
240. Tang, H. (2022). "Generating haar-uniform randomness using stochastic quantum walks on a photonic chip". *Phys. Rev. Lett.* **128**. doi:10.1103/PhysRevLett.128.050503.
241. Flamini, F. (2015). "Thermally reconfigurable quantum photonic circuits at telecom wavelength by femtosecond laser micromachining". *Light: Science & Applications* **4**. doi:10.1038/lsa.2015.127.
242. Polino, E. (2019). "Experimental multiphase estimation on a chip". *Optica* **6** (3): 288–295. doi:10.1364/OPTICA.6.000288.
243. Antón, C. (2019). "Interfacing scalable photonic platforms: solid-state based multi-photon interference in a reconfigurable glass chip". *Optica* **6** (12): 1471–1477. doi:10.1364/OPTICA.6.001471.
244. Pont, M. (2022). "Quantifying n-photon indistinguishability with a cyclic integrated interferometer". *Phys. Rev. X* **12**. doi:10.1103/PhysRevX.12.031033.
245. Hoch, F. (2022). "Reconfigurable continuously-coupled 3d photonic circuit for boson sampling experiments". *npj Quantum Information* **8** (1). doi:10.1038/s41534-022-00568-6.
246. Atzeni, S. (2018). "Integrated sources of entangled photons at the telecomwavelength in femtosecond-laserwritten circuits". *Optica* **5** (3): 311–314. doi:10.1364/OPTICA.5.000311.
247. Llewellyn, D. (2020). "Chip-to-chip quantum teleportation and multi-photon entanglement in silicon". *Nat. Phys.* **16** (2): 148–153. doi:10.1038/s41567-019-0727-x.
248. Paesani, S. (2019). "Generation and sampling of quantum states of light in a silicon chip". *Nat. Phys.* **15** (9): 925–929. doi:10.1038/s41567-019-0567-8.
249. Santagati, R. (2018). "Witnessing eigenstates for quantum simulation of hamiltonian spectra". *Science Advances* **4** (1). doi:10.1126/sciadv.aap9646.
250. Adcock, J.C. (2019). "Programmable four-photon graph states on a silicon chip". *Nat. Commun.* **10** (1). doi:10.1038/s41467-019-11489-y.
251. Vigliar, C. (2021). "Error-protected qubits in a silicon photonic chip". *Nat. Phys.* **17** (10): 1137–1143. doi:10.1038/s41567-021-01333-w.
252. Wang, J. (2014). "Gallium arsenide (GaAs) quantum photonic waveguide circuits". *Optics Communications* **327**: 49–55. doi:10.1016/j.optcom.2014.02.040.

reconfigurable 12-mode quantum photonic processor". *Materials for Quantum Technology* **1** (3). doi:10.1088/2633-4356/ac168c.
255. Autebert, C. (2016). "Integrated algaas source of highly indistinguishable and energy-time entangled photons". *Optica* **3** (2): 143–146. doi:10.1364/OPTICA.3.000143.
256. Olbrich, F. (2017). "Polarization-entangled photons from an InGaAs-based quantum dot emitting in the telecom c-band". *Appl. Phys. Lett.* **111** (13). doi:10.1063/1.4994145.
257. Reck, M. (1994). "Experimental realization of any discrete unitary operator". *Phys. Rev. Lett.* **73**: 58–61. doi:10.1103/PhysRevLett.73.58.
258. Clements, W.R. (2016). "Optimal design for universal multiport interferometers". *Optica* **3** (12): 1460–1465. doi:10.1364/OPTICA.3.001460.
259. Hadfield, R.H. (2009). "Single-photon detectors for optical quantum information applications". *Nat. Photonics* **3** (12): 696–705. doi:10.1038/nphoton.2009.230.
260. Gerrits, T. (2011). "Onchip, photon-number-resolving, telecommunication-band detectors for scalable photonic information processing". *Phys. Rev. A* **84**. doi:10.1103/PhysRevA.84.060301.
261. Semenenko, H. (2020). "Chip-based measurementdevice- independent quantum key distribution". *Optica* **7** (3): 238–242. doi:10.1364/OPTICA.379679.
262. Wei, Kejin; Li, Wei (2020). "High-Speed Measurement-Device-Independent Quantum Key Distribution with Integrated Silicon Photonics". *Physical Review X* **10**. doi:10.1103/PhysRevX.10.031030.
263. Raussendorf, R. (2001). "A one-way quantum computer". *Phys. Rev. Lett.* **86**: 5188–5191. doi:10.1103/PhysRevLett.86.5188.
264. Raussendorf, R. (2003). "Measurement-based quantum computation on cluster states". *Phys. Rev. A* **68**. doi:10.1103/PhysRevA.68.022312.
265. Briegel, H.J. (2009). "Measurement-based quantum computation". *Nat. Phys.* **5** (1): 19–26. doi:10.1038/nphys1157.
266. Rudolph, T. (2017). "Why i am optimistic about the silicon-photonic route to quantum computing". *APL Photonics* **2** (3). doi:10.1063/1.4976737.
267. Bourassa, J.E. (2021). "Blueprint for a Scalable Photonic Fault-Tolerant Quantum Computer". *Quantum* **5**. doi:10.22331/q-2021-02-04-392.
268. Lecun, Y., Bottou, L., Bengio, Y. & Haffner, P. Gradient-based learning applied to document recognition. *Proc. IEEE* **86**, 2278–2324 (1998). doi:10.1109/5.726791 (https://doi.org/10.1109/5.726791)
269. Krizhevsky, A., Sutskever, I. & Hinton, G. E. ImageNet classification with deep convolutional neural networks. *Commun. ACM* **60**, 84–90 (2017). doi:10.1145/3065386 (https://doi.org/10.1145/3065386)
Weissenborn, D., Zhai, X., Unterthiner, T., Dehghani, M., Minderer, M., Heigold, G., Gelly, S., Uszkoreit, J. & Houlsby, N. An Image is Worth 16x16 Words: Transformers for Image Recognition at Scale. In *International Conference on Learning Representations* (2021). arXiv:2010.11929 (https://arxiv.org/abs/2010.11929)
272. Rosenblatt, F. The perceptron: a probabilistic model for information storage and organization in the brain. *Psychol. Rev.* **65**, 386–408 (1958). doi:10.1037/h0042519 (https://doi.org/10.1037/h0042519)
273. Goodfellow, I., Bengio, Y. & Courville, A. *Deep Learning* (MIT Press, 2016).
274. Shastri, B. J. et al. Photonics for artificial intelligence and neuromorphic computing. *Nat. Photon.* **15**, 102–114 (2021). doi:10.1038/s41566-020-00754-y (https://doi.org/10.1038/s41566-020-00754-y)
275. Lin, X. et al. All-optical machine learning using diffractive deep neural networks. *Science* **361**, 1004–1008 (2018). doi:10.1126/science.aat8084 (https://doi.org/10.1126/science.aat8084)
276. Zuo, Y. et al. All-optical neural network with nonlinear activation functions. *Optica* **6**, 1132–1137 (2019). doi:10.1364/OPTICA.6.001132 (https://doi.org/10.1364/OPTICA.6.001132)
277. Colburn, S., Chu, Y., Shilzerman, E. & Majumdar, A. Optical frontend for a convolutional neural network. *Appl. Opt.* **58**, 3179–3186 (2019). doi:10.1364/AO.58.003179 (https://doi.org/10.1364/AO.58.003179)
278. Li, S. et al. All-optical image identification with programmable matrix transformation. *Opt. Express* **29**, 26474–26485 (2021). doi:10.1364/OE.433969 (https://doi.org/10.1364/OE.433969)
279. Luo, Y. et al. Computational imaging without a computer: seeing through random diffusers at the speed of light. *eLight* **2**, 4 (2022). doi:10.1186/s43593-022-00012-4 (https://doi.org/10.1186/s43593-022-00012-4)
280. McMahon, P. L. The physics of optical computing. *Nat. Rev. Phys.* **5**, 717–734 (2023). doi:10.1038/s42254-023-00645-5 (https://doi.org/10.1038/s42254-023-00645-5)
281. Lloyd, S., Mohseni, M. & Rebentrost, P. Quantum algorithms for supervised and unsupervised machine learning. arXiv:1307.0411 (2013).
282. Cai, X.-D. et al. Entanglement-based machine learning on a quantum computer. *Phys. Rev. Lett.* **114**, 110504 (2015). doi:10.1103/PhysRevLett.114.110504 (https://doi.org/10.1103/PhysRevLett.114.110504)
283. Benatti, F., Mancini, S. & Mangini, S. Continuous variable quantum perceptron. *Int. J. Quantum Inf.* **17**, 1941009 (2019).
284. Tacchino, F., Macchiavello, C., Gerace, D. & Bajoni, D. An artificial neuron implemented on an actual quantum processor. *Npj Quant. Inf.* **5**, 26 (2019). doi:10.1038/s41534-019-0140-4 (https://doi.org/10.1038/s41534-019-0140-4)
tps://doi.org/10.1088/2632-2153/abaf98)
286. Cerezo, M. et al. Variational quantum algorithms. *Nat. Rev. Phys.* **3**, 625–644 (2021). doi:10.1038/s42254-021-00348-9 (https://doi.org/10.1038/s42254-021-00348-9)
287. Cerezo, M., Larocca, M., García-Martín, D., Diaz, N. L., Braccia, P., Fontana, E., Rudolph, M. S., Bermejo, P., Ijaz, A., Thanasilp, S., Anschuetz, E. R. & Holmes, Z. Does provable absence of barren plateaus imply classical simulability? Or, why we need to rethink variational quantum computing. *Nature Communications* **16**, 7907 (2025). doi:10.1038/s41467-025-63099-6 (https://doi.org/10.1038/s41467-025-63099-6)
288. Senokosov, A., Sedykh, A., Sagingalieva, A., Kyriacou, B. & Melnikov, A. Quantum machine learning for image classification. *Mach. Learn. Sci. Technol.* **5**, 015040 (2024). doi:10.1088/2632-2153/ad2aef (https://doi.org/10.1088/2632-2153/ad2aef)
289. Steinbrecher, G. R., Olson, J. P., Englund, D. & Carolan, J. Quantum optical neural networks. *Npj Quantum Inf.* **5**, 60 (2019). doi:10.1038/s41534-019-0174-7 (https://doi.org/10.1038/s41534-019-0174-7)
290. Killoran, N. et al. Continuous-variable quantum neural networks. *Phys. Rev. Res.* **1**, 033063 (2019). doi:10.1103/PhysRevResearch.1.033063 (https://doi.org/10.1103/PhysRevResearch.1.033063)
291. Bartkiewicz, K. et al. Experimental kernel-based quantum machine learning in finite feature space. *Sci. Rep.* **10**, 12356 (2020). doi:10.1038/s41598-020-68911-5 (https://doi.org/10.1038/s41598-020-68911-5)
292. Sui, X., Wu, Q., Liu, J., Chen, Q. & Gu, G. A review of optical neural networks. *IEEE Access* **8**, 70773–70783 (2020). doi:10.1109/ACCESS.2020.2987333 (https://doi.org/10.1109/ACCESS.2020.2987333)
293. Zhang, A. et al. Quantum verification of NP problems with single photons and linear optics. *Light Sci. Appl.* **10**, 169 (2021). doi:10.1038/s41377-021-00608-4 (https://doi.org/10.1038/s41377-021-00608-4)
294. Stanev, D., Spagnolo, N. & Sciarrino, F. Deterministic optimal quantum cloning via a quantum-optical neural network. *Phys. Rev. Res.* **5**, 013139 (2023). doi:10.1103/PhysRevResearch.5.013139 (https://doi.org/10.1103/PhysRevResearch.5.013139)
295. Wood, C., Shrapnel, S. & Milburn, G. J. A Kerr kernel quantum learning machine. arXiv:2404.01787 (2024).
296. Hong, C. K., Ou, Z. Y. & Mandel, L. Measurement of subpicosecond time intervals between two photons by interference. *Phys. Rev. Lett.* **59**, 2044–2046 (1987). doi:10.1103/PhysRevLett.59.2044 (https://doi.org/10.1103/PhysRevLett.59.2044)

298. Sadana, S. et al. Near-100% two-photon-like coincidence-visibility dip with classical light and the role of complementarity. *Phys. Rev. A* **100**, 013839 (2019). doi:10.1103/PhysRevA.100.013839 (https://doi.org/10.1103/PhysRevA.100.013839)
299. Hiekkamäki, M. & Fickler, R. High-dimensional two-photon interference effects in spatial modes. *Phys. Rev. Lett.* **126**, 123601 (2021). doi:10.1103/PhysRevLett.126.123601 (https://doi.org/10.1103/PhysRevLett.126.123601)
301. Glorot, X. & Bengio, Y. Understanding the difficulty of training deep feedforward neural networks. In *Proc. Thirteenth International Conference on Artificial Intelligence and Statistics*, vol. 9, 249–256 (PMLR, 2010).
302. Neff, J., Athale, R. & Lee, S. Two-dimensional spatial light modulators: a tutorial. *Proc. IEEE* **78**, 826–855 (1990).
303. Zhang, Z., You, Z. & Chu, D. Fundamentals of phase-only liquid crystal on silicon (LCOS) devices. *Light Sci. Appl.* **3**, e213 (2014).
Twenty-First International Conference on Machine Learning, ICML '04, 23 (2004).
306. Morgillo, A. R. & Roncallo, S. Quantum optical neuron. GitHub (2025). https://github.com/simoneroncallo/quantum-optical-neuron (https://github.com/simoneroncallo/quantum-optical-neuron)

Operators in physics		
General	Space and time	d'Alembertian · Parity · Time
	Particles	C-symmetry
	Operators for operators	Anti-symmetric operator · Ladder operator
Quantum	Fundamental	Momentum · Position · Rotation
	Energy	Total energy · Hamiltonian · W:Kinetic energy
	Angular momentum	Total · Orbital · Spin
	Electromagnetism	Transition dipole moment
	Optics	Displacement · Hanbury Brown and Twiss effect · Out-of-time-ordered correlator · Squeeze
	Particle physics	Casimir invariant · Creation and annihilation

Category: Quantum optics, Optical components, Interferometry